

## INFORMATION TO USERS

This reproduction was made from a copy of a document sent to us for microfilming. While the most advanced technology has been used to photograph and reproduce this document, the quality of the reproduction is heavily dependent upon the quality of the material submitted.

The following explanation of techniques is provided to help clarify markings or notations which may appear on this reproduction.

1. The sign or "target" for pages apparently lacking from the document photographed is "Missing Page(s)". If it was possible to obtain the missing page(s) or section, they are spliced into the film along with adjacent pages. This may have necessitated cutting through an image and duplicating adjacent pages to assure complete continuity.
2. When an image on the film is obliterated with a round black mark, it is an indication of either blurred copy because of movement during exposure, duplicate copy, or copyrighted materials that should not have been filmed. For blurred pages, a good image of the page can be found in the adjacent frame. If copyrighted materials were deleted, a target note will appear listing the pages in the adjacent frame.
3. When a map, drawing or chart, etc., is part of the material being photographed, a definite method of "sectioning" the material has been followed. It is customary to begin filming at the upper left hand corner of a large sheet and to continue from left to right in equal sections with small overlaps. If necessary, sectioning is continued again—beginning below the first row and continuing on until complete.
4. For illustrations that cannot be satisfactorily reproduced by xerographic means, photographic prints can be purchased at additional cost and inserted into your xerographic copy. These prints are available upon request from the Dissertations Customer Services Department.
5. Some pages in any document may have indistinct print. In all cases the best available copy has been filmed.

**University  
Microfilms  
International**

300 N. Zeeb Road  
Ann Arbor, MI 48106



1327922

Anhalt, Dennis Paul

MODIFICATION OF A DIAGNOSTIC ULTRASOUND UNIT'S MOVEMENT  
SYSTEM TO PERFORM SCANNING DURING FOCUSSED, ULTRASOUND  
HYPERTHERMIA

*The University of Arizona*

M.S.

1986

University  
Microfilms  
International 300 N. Zeeb Road, Ann Arbor, MI 48106



MODIFICATION OF A DIAGNOSTIC ULTRASOUND UNIT'S MOVEMENT SYSTEM  
TO PERFORM SCANNING DURING FOCUSSED, ULTRASOUND HYPERTHERMIA

by

Dennis Paul Anhalt

---

A Thesis Submitted to the Faculty of the  
DEPARTMENT OF ELECTRICAL AND COMPUTER ENGINEERING

In Partial Fulfillment of the Requirements  
For the Degree of

MASTER OF SCIENCE  
WITH A MAJOR IN ELECTRICAL ENGINEERING

In the Graduate College  
THE UNIVERSITY OF ARIZONA

1 9 8 6

STATEMENT BY AUTHOR

This thesis has been submitted in partial fulfillment of requirements for an advanced degree at The University of Arizona and is deposited in the University Library to be made available to borrowers under rules of the Library.

Brief quotations from this thesis are allowable without special permission, provided that accurate acknowledgment of source is made. Requests for permission for extended quotation from or reproduction of this manuscript in whole or in part may be granted by the head of the major department or the Dean of the Graduate College when in his or her judgment the proposed use of the material is in the interests of scholarship. In all other instances, however, permission must be obtained from the author.

SIGNED: Dennis P. Anhalt

APPROVAL BY THESIS DIRECTOR

This thesis has been approved on the date shown below:

Robert B. Roemer  
R. B. ROEMER  
Associate Professor of Aerospace  
and Mechanical Engineering

4/15/86  
Date

## ACKNOWLEDGMENTS

The author would like to express sincere thanks to the following individuals who made this project possible: Dr. Kenneth C. Mylrea and Dr. Robert B. Roemer for their constant advice and encouragement and to Dr. Kullervo Hynynen, Eugene J. Gross, Charles A. Johnson, Chris J. Diederich, Eduardo Moros, and Anne E. Fletcher who provided friendship, technical support and advice for the duration of this work. The author would also like to thank the Ausonics Corporation, Australia, for donating major equipment for use in this study and for providing technical support.

The author would like to give greatest thanks to his parents, Edward and Clara Anhalt, for without their love, encouragement and constant support, this project and many which came before it would not have been possible.

This research has been supported by NCI grant CA33922-02.

## TABLE OF CONTENTS

	Page
LIST OF TABLES . . . . .	vi
LIST OF ILLUSTRATIONS . . . . .	viii
ABSTRACT . . . . .	x
1. INTRODUCTION . . . . .	1
2. MOVEMENT SYSTEM DESCRIPTION . . . . .	7
2.1 Principle of Operation of the Octoson® . . . . .	7
2.2 Hardware . . . . .	10
2.2.1 HP Computer/Octoson® Movement System Interface. . . . .	10
2.2.2 Apple IIe - Anaheim Indexers/Octoson® Movement System Interface . . . . .	16
2.2.3 Safety Hardware . . . . .	24
2.3 Software . . . . .	24
2.3.1 HP/Octoson® Interface Software . . . . .	26
2.3.2 Apple IIe - Anaheim Indexers/Octoson® Interface Software . . . . .	28
3. SYSTEM CALIBRATIONS AND RELIABILITY TESTS . . . . .	39
3.1 Octoson® Positioning Repeatability . . . . .	39
3.2 Indexer Calibrations . . . . .	45
3.3 Movement System Overshoot . . . . .	46
3.3.1 X Direction Overshoot . . . . .	48
3.3.2 Y Direction Overshoot . . . . .	52
3.3.3 Z Direction Overshoot . . . . .	55
3.3.4 R Direction Overshoot . . . . .	58
3.3.5 T Direction Overshoot . . . . .	58
3.3.6 Summary of Movement System Overshoot Studies. . . . .	61



TABLE OF CONTENTS--Continued

	Page
3.4 Maximum Speeds Attainable . . . . .	62
3.5 Reliability Tests . . . . .	66
3.6 Safety Potentiometer Calibration . . . . .	66
4. DISCUSSION . . . . .	72
APPENDIX A: INDEXER COMMANDS AND EXAMPLES . . . . .	74
A.1 Command Descriptions . . . . .	75
A.2 Other Useful Indexer Information and Examples . . . . .	77
APPENDIX B: SYSTEM IDIOSYNCRASIES . . . . .	80
APPENDIX C: SUMMARY OF RESULTS OF <u>IN VIVO</u> EXPERIMENTS . . . . .	83
REFERENCES . . . . .	85

## LIST OF TABLES

Table	Page
1. Equipment Used . . . . .	3
2. Octoson® "As Is" Speeds and Oscillator Frequencies . . . . .	11
3. HP Computer/Octoson® Interface Connections . . . . .	14
4. HP Channels Used to Measure Position Voltages . . . . .	15
5. Apple IIe - Anaheim Indexers/Octoson® Interface Circuit Board Wire Connections . . . . .	19
6. Indexers Hard Limit Switch Connections . . . . .	22
7. Apple IIe A/D Channels Used to Monitor Safety Potentiometers . . . . .	25
8. Program Names and Descriptions . . . . .	38
9. Displacement (in mm) From Previous Position due to Repeated Power Off/On Sequences . . . . .	41
10. Displacement (in mm) From Previous Position due to Repeated Initializations . . . . .	42
11. Displacement (in mm) From Previous Position due to Initialization Following Power On . . . . .	43
12. Displacement (in mm) From Previous Position due to Power Off/On Following Initialization . . . . .	44
13. Indexer Calibration Data . . . . .	47
14. Maximum Speeds Attainable Before Loss of Motor Synchronization is Instantly Noticed . . . . .	64
15. Maximum Speeds Attainable Before Loss of Motor Synchronization is Noticed With Time . . . . .	65

LIST OF TABLES--Continued

Table	Page
16. X Direction Safety Potentiometer Calibration Data . . . . .	68
17. Y Direction Safety Potentiometer Calibration Data . . . . .	69
18. Z Direction Safety Potentiometer Calibration Data . . . . .	70
19. Safety Potentiometer Calibration Summary . . . . .	71
A.1. Anaheim Indexers Rate Number/Speed Cross Reference . . . . .	79

## LIST OF ILLUSTRATIONS

Figure	Page
1. System Block Diagram . . . . .	4
2. Movement System Block Diagram . . . . .	8
3. Octoson® Positioning Circuitry . . . . .	9
4. HP Computer/Octoson® Interface "Break-Out" Box and Switching . . . . .	13
5. Apple IIe - Anaheim Indexers/Octoson® Interface Circuit Diagram . . . . .	18
6. Indexer Delay Circuit . . . . .	23
7. HP Octagonal Scanning Pattern . . . . .	27
8. Simplified Program Flowchart for the HP Octagonal Scanning Pattern . . . . .	29
9. Copy of an Actual Trace of the Apple IIe - Anaheim Indexers Octagonal Scanning Pattern . . . . .	30
10. Copy of an Actual Trace of the Apple IIe - Anaheim Indexers Raster-Filled Circular Scanning Pattern . . . . .	31
11. Exemplatory Sketches of the Apple IIe - Anaheim Indexers Elongated Octagonal Scanning Pattern . . . . .	33
12. Simplified Program Flowchart for the Apple IIe - Anaheim Indexers Octagonal Scanning Pattern . . . . .	34
13. Simplified Program Flowchart for the Apple IIe - Anaheim Indexers Raster-Filled Circular Scanning Pattern . . . . .	35
14. X Direction Overshoot as a Function of Base Speed and Z Position . . . . .	49

LIST OF ILLUSTRATIONS--Continued

Figure	Page
15. X Direction Overshoot as a Function of Maximum Speed, Acceleration, Deceleration, and Z Position . . . . .	51
16. Y Direction Overshoot as a Function of Base Speed and Z Position . . . . .	53
17. Y Direction Overshoot as a Function of Maximum Speed, Acceleration, Deceleration, and Z Position . . . . .	54
18. Z Direction Overshoot as a Function of Base Speed . . . . .	56
19. Z Direction Overshoot as a Function of Maximum Speed, Acceleration, and Deceleration . . . . .	57
20. T Direction Overshoot as a Function of Base Speed . . . . .	59
21. T Direction Overshoot as a Function of Maximum Speed, Acceleration, and Deceleration . . . . .	60
B.1. Data Format of the Anaheim Indexer RS 232 Interface . . . . .	82

## ABSTRACT

As a modality to induce hyperthermia for cancer treatment, scanned, focussed ultrasound is presently receiving much attention. A major area of investigation involves determining optimal methods of scanning the focussed beams. For this research, a commercial diagnostic ultrasound system incorporating mechanical scanning has been modified to provide good therapeutic scanning versatility, thus allowing the clinician to control size, pattern and speed of the scan. Calibrations performed on the system include overshoot as a function of scanning parameters, maximum speeds attainable, and distance traveled per motor step. Reliability tests performed consisted of scanning a given pattern for several hours at a time to determine how accurately the pattern repeated itself. The results indicate that mechanical scanning of focussed ultrasound beams may be a feasible method for effectively inducing hyperthermia for cancer treatment. The development of the system is described, and results of calibrations and other tests are presented.

## CHAPTER 1

### INTRODUCTION

Until recently, research involving hyperthermia used simple heating methods such as water bath immersion, single applicator microwaves or radiofrequency. Strohbehn and Douple [1] give an excellent history and overview of hyperthermia as a modality for cancer treatment from an engineer's perspective, including a description of existing heating modalities. As the limitations of early techniques became evident, investigations into other techniques for inducing hyperthermia progressed, and advances have been made. It is now possible to deposit energy into the body in several ways. Techniques presently under investigation include, but are not limited to, magnetic induction [2-4], multiple aperture microwaves [4-6], resonant helical coils [6-8], ferromagnetic implants [3,9], and ultrasound [10-12]. Each technique has associated with it certain advantages and disadvantages which may differ from other techniques. Therefore, it is speculated that each technique will complement the others in a cancer treatment center or environment.

This study is concerned with scanned, focussed ultrasound, a method to induce hyperthermia which was first introduced by Dr. P. P. Lele in 1975 [10]. Since that time, investigation into the optimal methods of focussing and scanning the ultrasound beams has

continued. Methods of focussing ultrasonic energy include lenses, mirrors, and concave transducers. Scanning of the ultrasonic focus is accomplished either electrically or mechanically.

In electrical scanning, the ultrasonic focus of an array of ultrasound transducers is moved around and/or throughout a treatment volume by electronically steering the ultrasound beams. In mechanical scanning, a focussed, ultrasound transducer, or an array of focussed ultrasound transducers all focussed at a known point (or points), is moved around and/or throughout a treatment volume by mechanical means (e.g., stepper motors and the necessary hardware and software). Although electrical scanning has received recent attention [12], in general it has not yet been studied enough to understand its potentials and limitations.

This study utilizes mechanical scanning as a method for moving the ultrasonic focus (or foci, when using multiple transducers which do not share a common focal point) to induce hyperthermia. For this investigation, a commercial diagnostic ultrasound scanner (the Octoson®) was modified to become a hyperthermia treatment system. This provides the capability of imaging the tissue volume prior to treatment and allows utilization of an existing mechanical movement system. Table 1 is a list of equipment used, and Figure 1 presents a block diagram of the system. Refer to Figure 1 for the following system description.



Table 1. Equipment Used

---

Octoson® diagnostic ultrasound B-scanner manufactured by Ausonics Pty. Ltd., Australia
Hewlett Packard, Incorporated, Model 9836 desktop computer
Hewlett Packard, Incorporated, Model 3497 data acquisition system
Hewlett Packard, Incorporated, Model 3456 digital voltmeter
URI Therm-X, Incorporated, Model L-500 power amplifiers
Apple, Incorporated, Apple IIe computer
Anaheim Automation, Incorporated, Model 1397 and Model 1408 programmable stepper motor indexers
Therapeutic transducers manufactured by Ausonics Pty. Ltd., Australia
Thermocouples fabricated in-house
Impedance matching network fabricated in-house

---

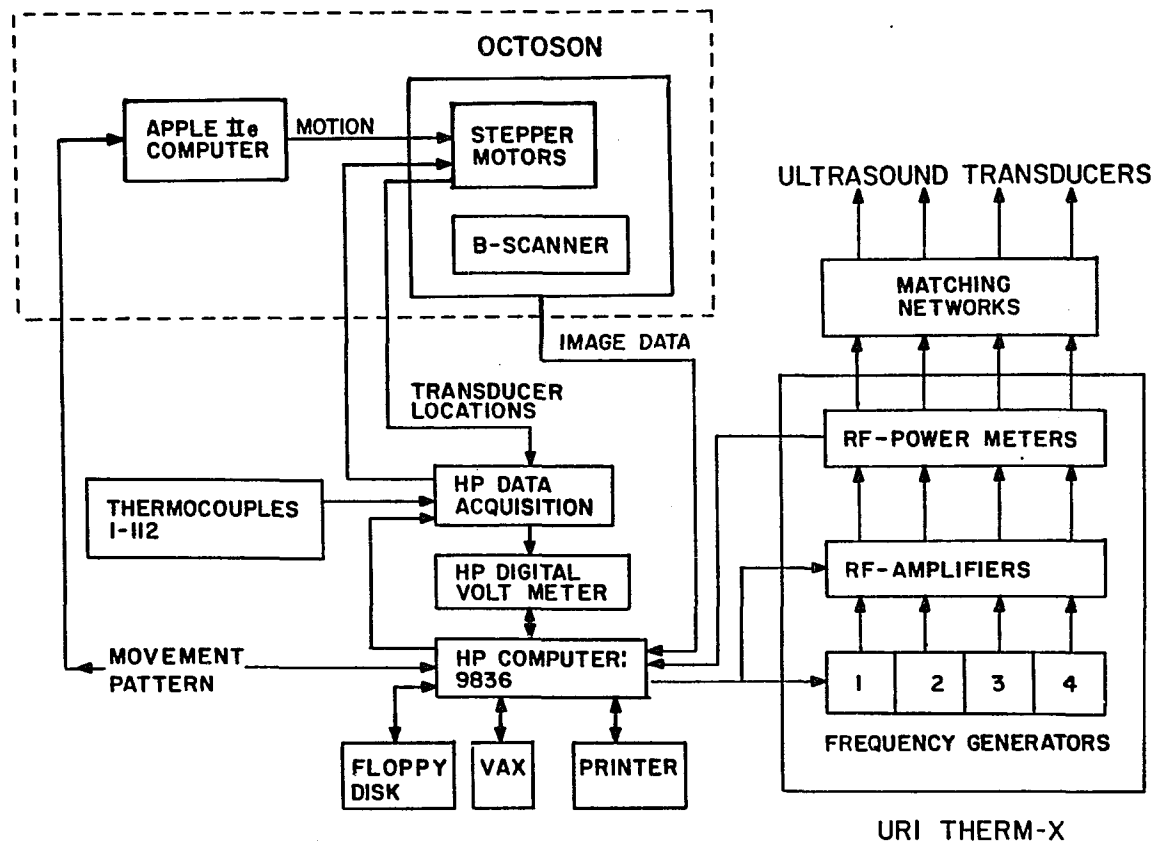


Figure 1. System Block Diagram

The Octoson®, a commercial ultrasound B-scanner, has eight focussed, diagnostic, ultrasound transducers mounted in a circular arc on a gantry that can be moved in X, Y, and Z directions and can be rotated (R) and tilted (T). A major modification to the Octoson® was the mounting of four high-power, focussed, ultrasound transducers (therapeutic transducers) on the gantry, two on each side of the diagnostic transducer arc. The mounting hardware allows for individual adjustment of each therapy transducer. For example, all four can be adjusted to share a common focus or, on the other hand, each can be adjusted to give a total of four distinct foci, or any combination in between. Once the focal arrangement of the four therapy transducers is chosen, the transducers are fixed in position for the duration of the treatment. The therapy transducers are driven via URI Therm-X, Incorporated, power amplifiers. The whole transducer assembly is submersed in a 273 gallon water bath, on top of which the patient lies during treatment.

Other major modifications to the diagnostic unit included the addition of a computerized data acquisition and control system, and a computerized motor control system. The data acquisition system is capable of measuring up to 112 thermocouples, thus enabling comprehensive temperature monitoring of tissue volumes during treatments. Special interfaces were designed and constructed which enable the transfer of image data to the HP computer, and allow either the HP computer or the Apple IIe computer to control the transducer movement system, and hence scanning of the therapeutic focus.

This thesis presents a compilation of the process of modifying the Octoson® unit's movement system (dashed, rectangular enclosure in Figure 1) including descriptions of the necessary hardware and software developed to perform therapeutic scanning under computer control, and calibrations and tests done to accurately predict the behavior of the system during scanning. The newly developed system shall allow continued investigation of scanned, focussed ultrasound as a modality for inducing hyperthermia for cancer treatment.

## CHAPTER 2

### MOVEMENT SYSTEM DESCRIPTION

This chapter describes the transducer movement system (Figure 2) in detail. The principle of operation of the Octoson's® movement system will be described, along with descriptions of the hardware interfaces which were designed and constructed to allow the external computers to control therapeutic scanning. The system software that was written to control therapeutic scanning will also be described, with flowcharts used to aid description where appropriate. A complete set of well-documented programs remains with the computer and is readily available for reference.

#### 2.1 Principle of Operation of The Octoson®

The Octoson® provides five degrees of freedom for positioning the transducer gantry; three translational directions (X, Y, and Z) and two angular directions - rotate (R) and tilt (T). The gantry position is controlled via five potentiometers mounted on the front panel of the Octoson® console. The positioning circuitry (Figure 3) utilizes voltage controlled oscillators/comparators and transistor drivers to step the motors, and binary counters and D/A converters as a type of pseudo feedback. As a potentiometer is varied, the oscillator outputs a pulse train and movement begins. Movement continues until the counter - D/A voltage equals the position

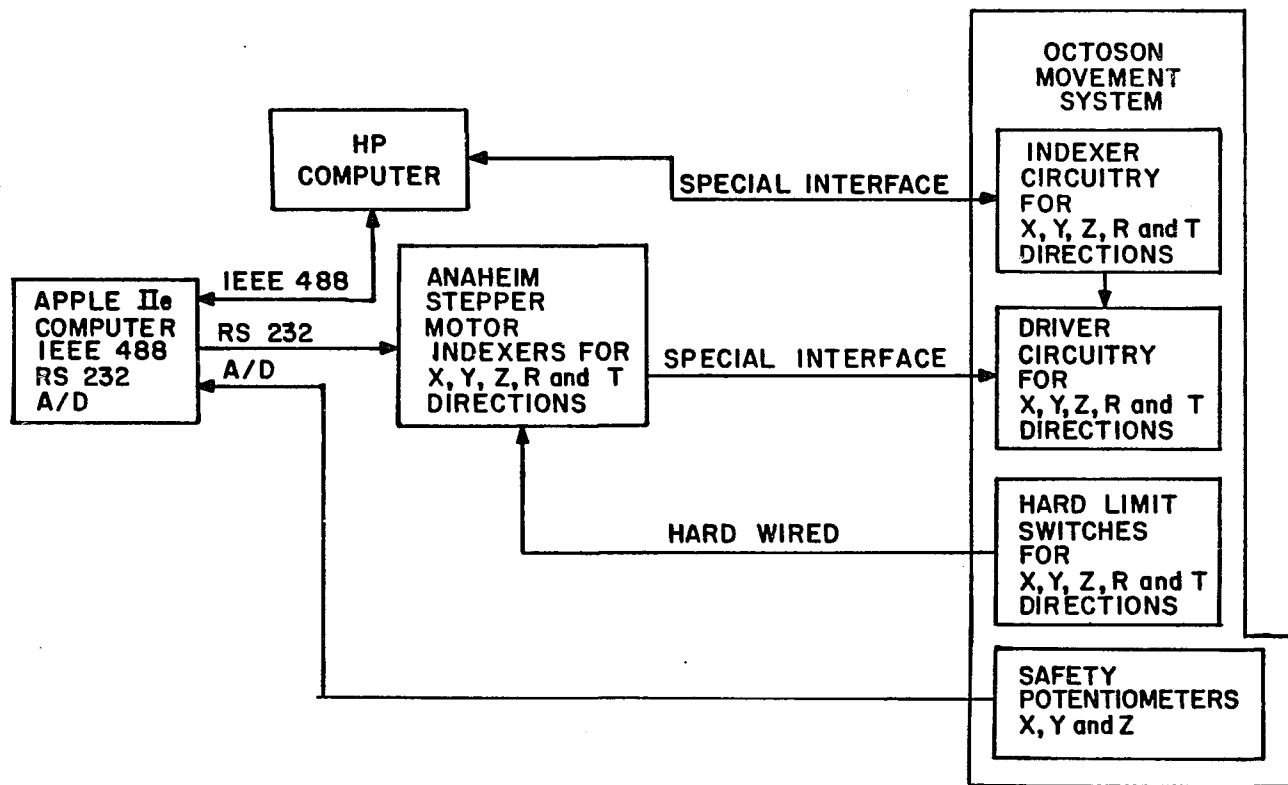


Figure 2. Movement System Block Diagram

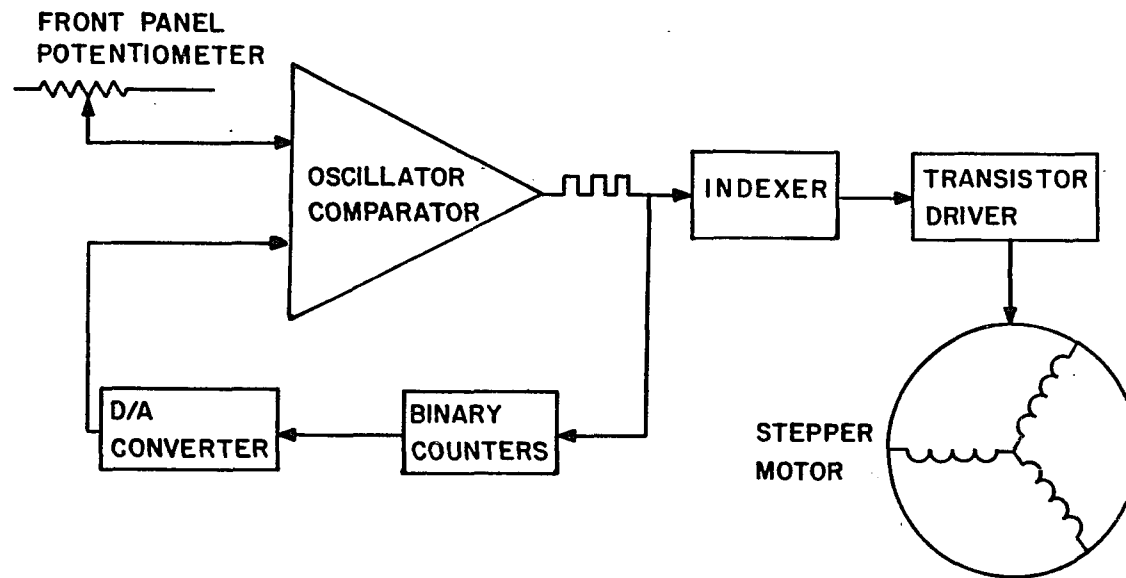


Figure 3. Octoson Positioning Circuitry

potentiometer voltage, at which time oscillations and hence movement cease. I chose to call this pseudo feedback because in the event that movement mechanics cause a motor to slip, the counters can only assume the motor is moving the gantry to the desired location. Therefore, the Octoson® movement system is actually open loop. The speed of travel in each direction is given in Table 2, and is referred to as the "as is" speed throughout this thesis.

## 2.2 Hardware

### 2.2.1 HP Computer/Octoson® Movement System Interface

The HP system has available several channels to be used as input for measuring voltages, and four channels of D/A output capable of supplying -10.23 to +10.23 volts in 2.5 millivolt increments. (It was thought that by these mechanisms the HP could measure gantry position voltages and then output a sequence of analog voltages to control therapeutic scanning.) The D/A output channels act to replace the positioning potentiometers on the front panel of the Octoson® console during therapeutic scanning. (Because only four channels of D/A output are available, one direction needed to be excluded from this interface. It was thought that the tilt direction would be the least beneficial during therapeutic scanning, and therefore it was excluded.) The 2.5 millivolts resolution of the HP D/A output channels corresponds to an incremental resolution of 0.17 millimeters in the three translational directions and 0.18 degrees in the rotate direction. The voltage range of the D/A output channels is sufficient to move the gantry through its limits in all directions.



Table 2. Octoson® "As Is" Speeds and Oscillator Frequencies

Direction	Speed	Frequency
X	14 mm/s	240 Hz
Y	12 mm/s	270 Hz
Z	10 mm/s	680 Hz
R	5 deg/s	240 Hz
T	4 deg/s	390 Hz

To give control of the Octoson's® movement system to the HP system a "break-out" box (Figure 4) was built which simply switches out the front panel position potentiometers and switches in the HP D/A output channels. The "break-out" box consists of a four-pole double-throw relay and a switching transistor, with the actual switching controlled via a TTL line from the HP computer. The interface connections are through a 25 conductor cable and are given in Table 3. Figure 4 indicates which HP D/A output channels are used for each direction and Table 4 indicates which HP input channels are used for measuring gantry position voltages. The position voltages are measured at the output of the D/A of the Octoson® positioning circuitry.

The major information obtained from using this interface for therapeutic scanning was that greater flexibility was needed in the movement system. The effectiveness of therapeutic scanning would be enhanced if the operator could control the speed, acceleration, and deceleration used during the scan. Although this interface is no longer used for therapeutic scanning, it is used for locating thermocouples which have been inserted into the tissue volume prior to treatment.

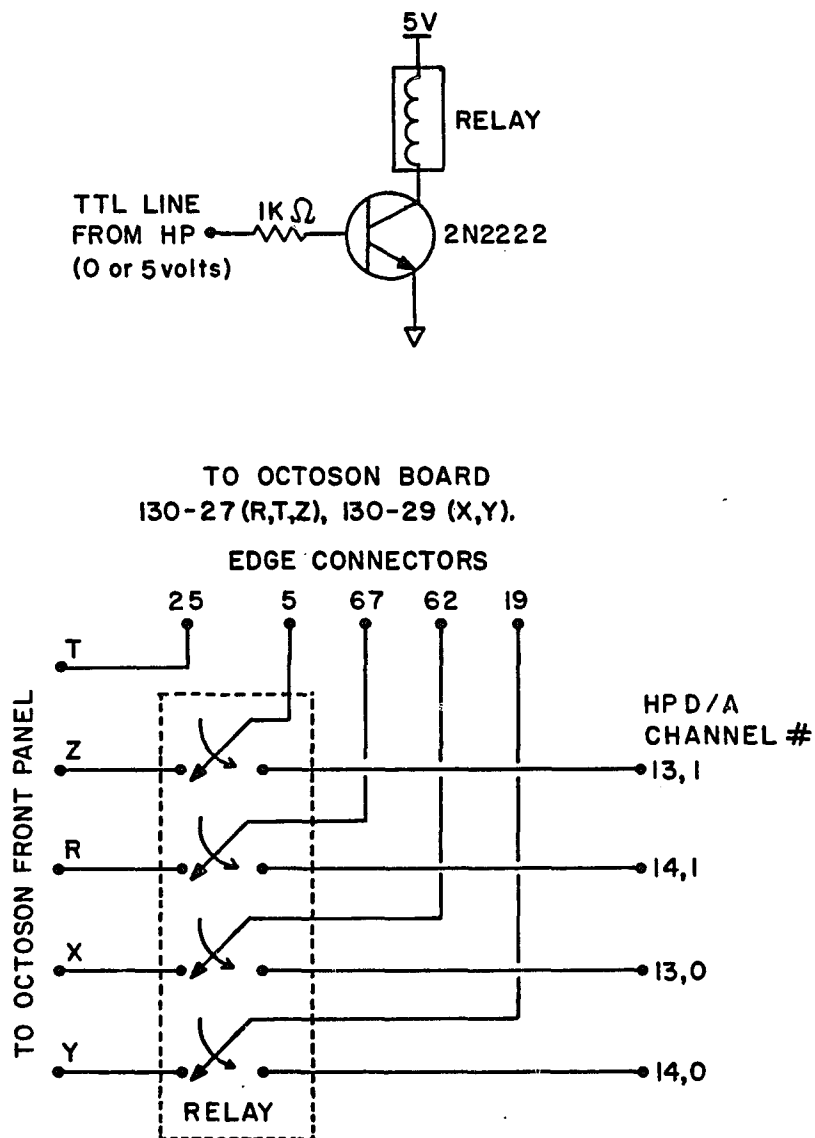


Figure 4. HP Computer/Octoson® Interface "Break-Out" Box and Switching

Table 3. HP Computer/Octoson® Interface Connections

25 Conductor Cable Connector Pin Number	Description
1	Y D-A high output to edge connector 19 (130-29)
2	Y Low sense
3	R D-A high output to edge connector 67 (130-27)
4	R Low sense
5	X D-A high output to edge connector 62 (130-29)
6	X Low sense
7	Z D-A high output to edge connector 05 (130-27)
8	Z Low sense
9	X Measure from edge connector 64 (130-29)
10	Z Measure from edge connector 07 (130-27)
11	T Measure from edge connector 27 (130-27)
12	Ground
13	No connection
14	Y High sense
15	Y Low (Gnd)
16	R High sense
17	R Low (Gnd)
18	X High sense
19	X Low (Gnd)
20	Z High sense
21	Z Low (Gnd)
22	Y Measure from edge connector 07 (130-29)
23	R Measure from edge connector 65 (130-27)
24	Ground
25	No Connection

Note: (nnn-nn) Indicates Octoson® Printed Circuit Board Number

Table 4. HP Channels Used to Measure Position Voltages

Direction	HP Channel Number
X	60
Y	61
Z	62
R	63
T	64

### 2.2.2 Apple IIe - Anaheim Indexers/Octoson® Movement System Interface

The motivation for building this interface was versatility; an attribute the Octoson® lacked (i.e., movement was at a fixed rate and fixed acceleration and deceleration). Programmable stepper motor indexers alleviate these constraints. The system to be described is the main system used to drive the transducer gantry during therapeutic scanning.

It is felt that the word indexer requires defining. Typically a stepper motor controller has two distinct portions - a driver and an indexer. The driver portion, consisting primarily of high current power supplies and high current switching transistors, operates only when instructed to by the indexer portion, and in the manner prescribed by the indexer. The indexer, on the other hand, is responsible for all of the logic (typically TTL) and communication necessary to control the driver. Because the driver contains mainly power supplies and transistors, its circuitry is normally not very complex. However, the indexer circuitry can range from simple to very complex depending on its overall versatility, with increased complexity coincident with increased versatility.

An indication of the versatility of the indexers used for this study can be obtained from the following attributes particular to them. The indexers provide soft and hard limit inputs, which are necessary. They allow the operator to specify base rate (the speed at which motion begins and ends at), maximum rate (the fastest speed of travel during a move), acceleration characteristic (the rate of

increase from base rate to maximum rate), deceleration characteristic (the rate of decrease from maximum rate to base rate), and the length and direction of travel. The indexers also have available 75 bytes of memory and trigger inputs and outputs, which allow them to operate in deferred execution mode. For example, upon completion of a move, an indexer triggers one or more other indexers (with previously entered command strings) to begin movement. The completion of this move may in turn trigger other indexers to begin movement. The combinations are many and are limited only by memory constraints. Deferred execution may prove useful once certain scanning patterns particular to specific treatment protocols become established. However, to this date deferred execution has received little attention. A complete list of indexer commands is given in Appendix A, along with example calculations and command strings.

A total of six indexers are available, thus providing one spare. One indexer (Model 1397) has a standard RS 232 interface to communicate with the Apple IIe, and other indexers (Model 1408) are connected to the previous one in a daisy chain fashion via parallel interfaces. Up to six axes can be daisy chained, therefore satisfying the axes needs of the Octoson® movement system.

The circuit shown in Figure 5 was designed and constructed, and wired into the existing Octoson® driver circuitry. Table 5 indicates the interface wire connections, i.e., from which Octoson® printed circuit board edge connectors to which edge connectors of the newly constructed circuit board. The only additional wiring done was

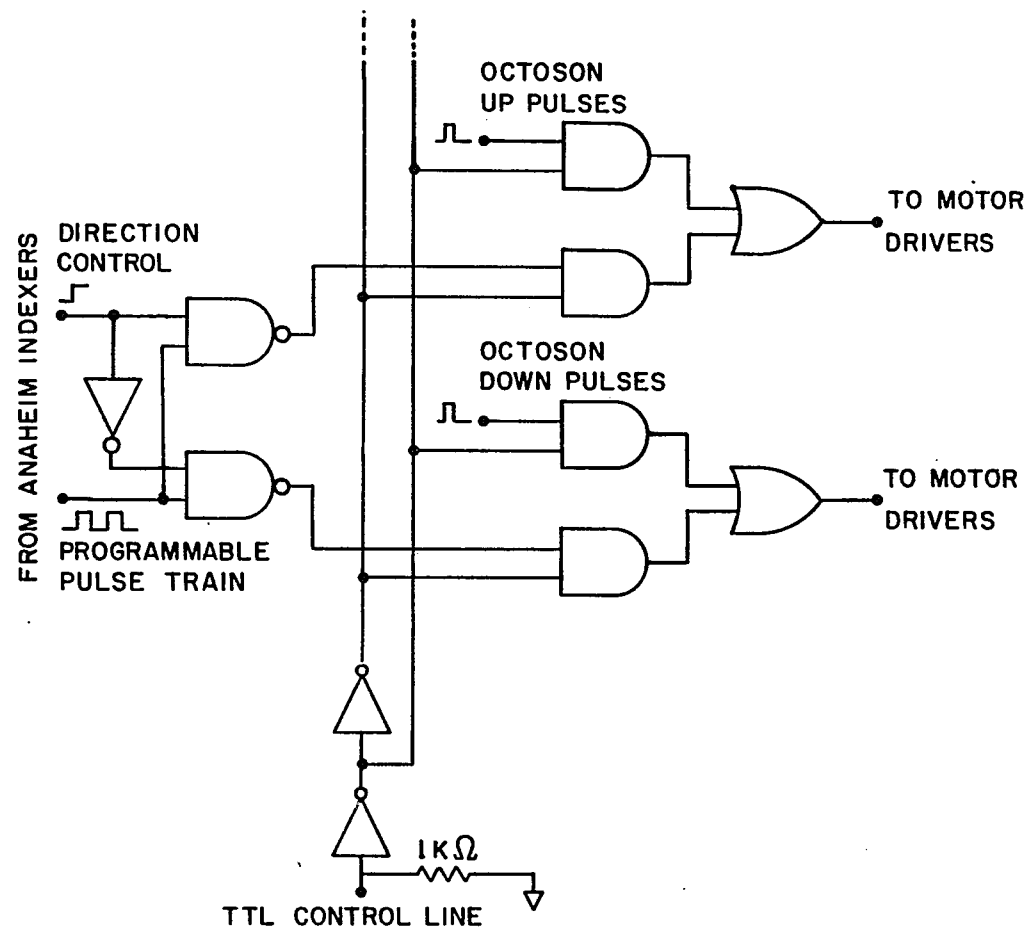


Figure 5. Apple IIe - Anaheim Indexers/Octoson® Interface Circuit Diagram



Table 5. Apple IIe - Anaheim Indexers/Octoson  
Interface Circuit Board Wire Connections

Edge Connector Number	Description
Lower Portion (Indexers)	
1	+5 volts
2	Ground
25	X Indexer direction control
26	X Indexer pulse train
27	X Up pulses from Octoson® edge connector 50 (130-29)
28	X Down pulses from Octoson® edge connector 52 (130-29)
29	X Up pulses to edge connector 54 (130-29)
30	X Down pulses to edge connector 56 (130-29)
31	Y Indexer direction control
32	Y Indexer pulse train
33	Y Up pulses from Octoson® edge connector 31 (130-29)
34	Y Down pulses from Octoson® edge connector 33 (130-29)
36	Y Up pulses to edge connector 31 (130-21)
38	Y Down pulses to edge connector 33 (130-21)
40	Z Indexer direction control
42	Z Indexer pulse train
44	Z Up pulses from Octoson® edge connector 14 (130-27)
45	Z Down pulses from Octoson® edge connector 06 (130-27)
46	Z Up pulses to edge connector 13 (130-21)
48	Z Down pulses to edge connector 36 (130-21)
50	R Indexer direction pulses
51	R Indexer pulse train
52	R Up pulses from Octoson® edge connector 64 (130-27)
54	R Down pulses from Octoson® edge connector 63 (130-27)
56	R Up pulses to edge connector 63 (130-22)
58	R Down pulses to edge connector 57 (130-22)
59	T Indexer direction control
60	T Indexer pulse train
62	T Up pulses from Octoson® edge connector 30 (130-27)
63	T Down pulses from Octoson® edge connector 60 (130-27)
64	T Up pulses to edge connector 29 (130-22)
66	T Down pulses to edge connector 59 (130-22)
68	Apple IIe control, annunciator 0 (RS 232 cable pin 1)

Note: (nnn-nn) Indicates Octoson® Printed Circuit Board Number

Table 5. Continued

Edge Connector Number	Description
Upper Portion (Amplifiers)	
5	Coaxial cable from HP Computer
7	Apple IIe control, annunciator 1 (RS 232 cable pin 25)
8	Coaxial cable to Wavetek and in turn to Amplifiers

to connect the Octoson's® hard limit switches to the hard limit inputs of the respective indexer for each direction, and is given in Table 6.

When indexers are daisy chained, the indexers on the daisy chain must reach their power on state before the indexer containing the RS 232 interface does. This allows the indexer containing the RS 232 interface to see if other indexers are available to receive instructions. The delay circuit in Figure 6 was built to ensure sufficient delay for the indexer containing the RS 232 interface. The reason for a transistor in the delay circuit instead of a simple RC delay is because the indexers sink up to one ampere of current per board. Therefore, any resistor in series with an indexer causes too large of voltage drop to allow the indexer's five volt regulators to function properly.

The power switch for the circuit is mounted on the front panel of the Octoson®, and should be in the off position when powering on the Octoson®. The indexers should be switched on only after the Octoson® completes its initialization process. This is to prevent improper power on of the indexers due to electrical transients which are present during the Octoson's® power on phase.

Table 6. Indexers Hard Limit Switch Connections

Indexer Hard Limit Direction	Octoson® Circuit Board (130-36) Edge Connector
+ X	54
- X	52
+ Y	56
- Y	58
+ Z	12
- Z	8
+ R	28
- R	30
+ T	26
- T	24

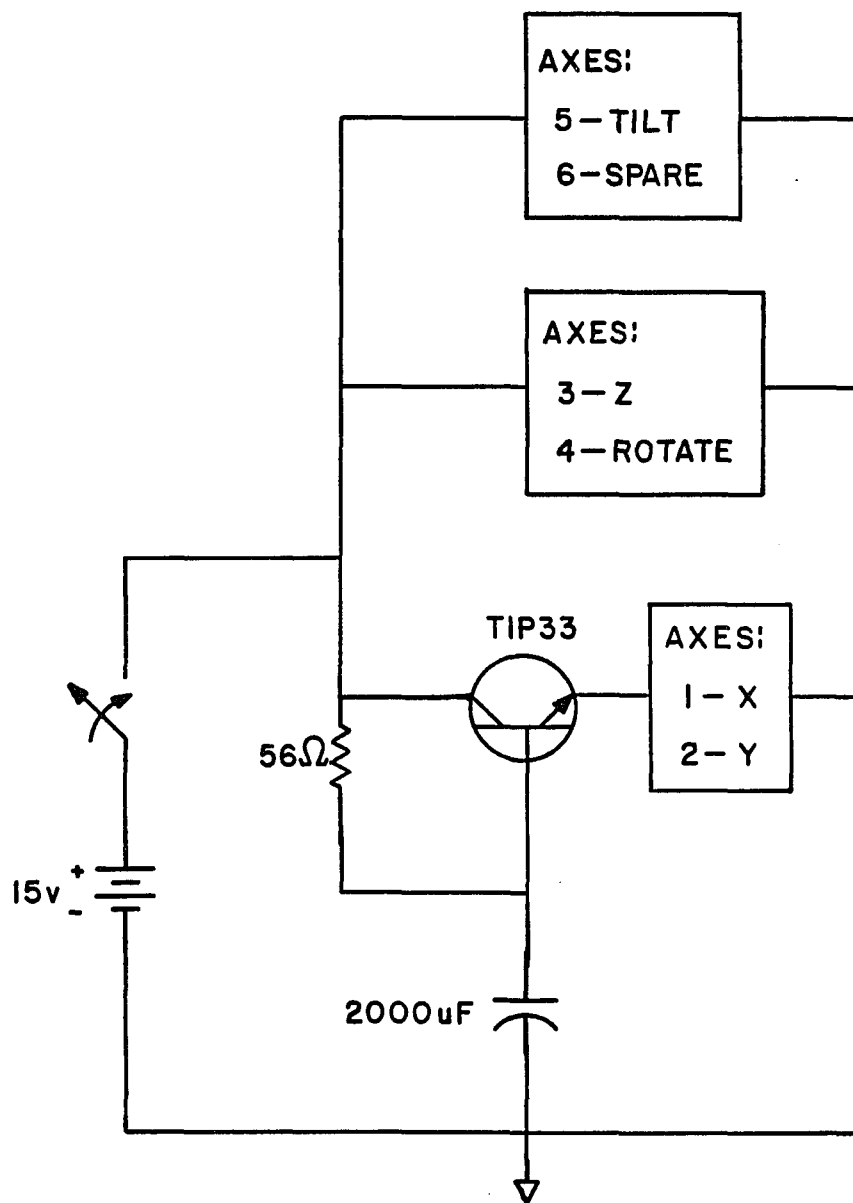


Figure 6. Indexer Delay Circuit

### 2.2.3 Safety Hardware

To obtain a true closed loop movement system, feedback potentiometers were mounted on the gantry for X, Y, and Z directions. They function to indicate whether or not the motors are moving the gantry to the programmed locations. The potentiometers are monitored by the Apple IIe via its 12 bit A/D interface card, with the wire connections given in Table 7. The rotate and tilt directions have yet to be used for therapeutic scanning, and therefore the addition of feedback potentiometers for these directions was postponed.

It was necessary to give the Apple IIe the authority to cut power to the therapeutic transducers, in the event the gantry fails to move or moves to an other than programmed location. The circuit is very simply an AND gate, and is part of the newly constructed circuit board. The wire connections are given in Table 5. Should the Apple IIe detect that the gantry position is not within a certain range of the programmed value, power to the therapeutic transducers is shut down in a matter of microseconds.

## 2.3 Software

As mentioned in the introductory paragraph of this chapter, flowcharts and descriptions will provide sufficient understanding of the software developed, and therefore program listings have been excluded. Again, all programs are with the computer for reference. It should be noted that the software used for driving the motors via the HP/Octoson® interface is similar to the software used for driving

Table 7. Apple IIe A/D Channels Used to Monitor Safety Potentiometers

Safety Potentiometer	Apple IIe A/D Channel Number	25 Conductor Cable Connector Pin Number
X	0	1
Y	1	2
Z	2	3
	Ground	25

the motors via the Apple IIe - Anaheim Indexers/Octoson® interface. However, because the HP programs are written to use millivolts per millimeters and the Apple IIe programs are written to use pulses per millimeter, individual discussion may help to better understand each.

### 2.3.1 HP/Octoson® Interface Software

The scanning pattern chosen was an octagon (Figure 7) for the main reason that once a voltage is output, the HP computer has time for other tasks. Longer straight-line segments allow the HP more time. If the pattern were more circular, i.e., many more, but shorter straight-line segments, the HP would be spending more time outputting voltages and have less time for other tasks.

The actual scan (Figure 7) is not a true octagon in that all sides are equal length for the following two reasons. First, for simplicity the total diameter is divided into thirds, with the diagonal-line segments connecting the inner thirds of all sides. Therefore, the diagonal-line segments are actually the square root of two times longer than the other line segments. Because the speed of travel for each direction is fixed, the scanning speed along the diagonal-line segments is approximately the square root of two times faster than the speed of travel during the other line segments; indicating that constant scanning speeds are not possible when using this interface.



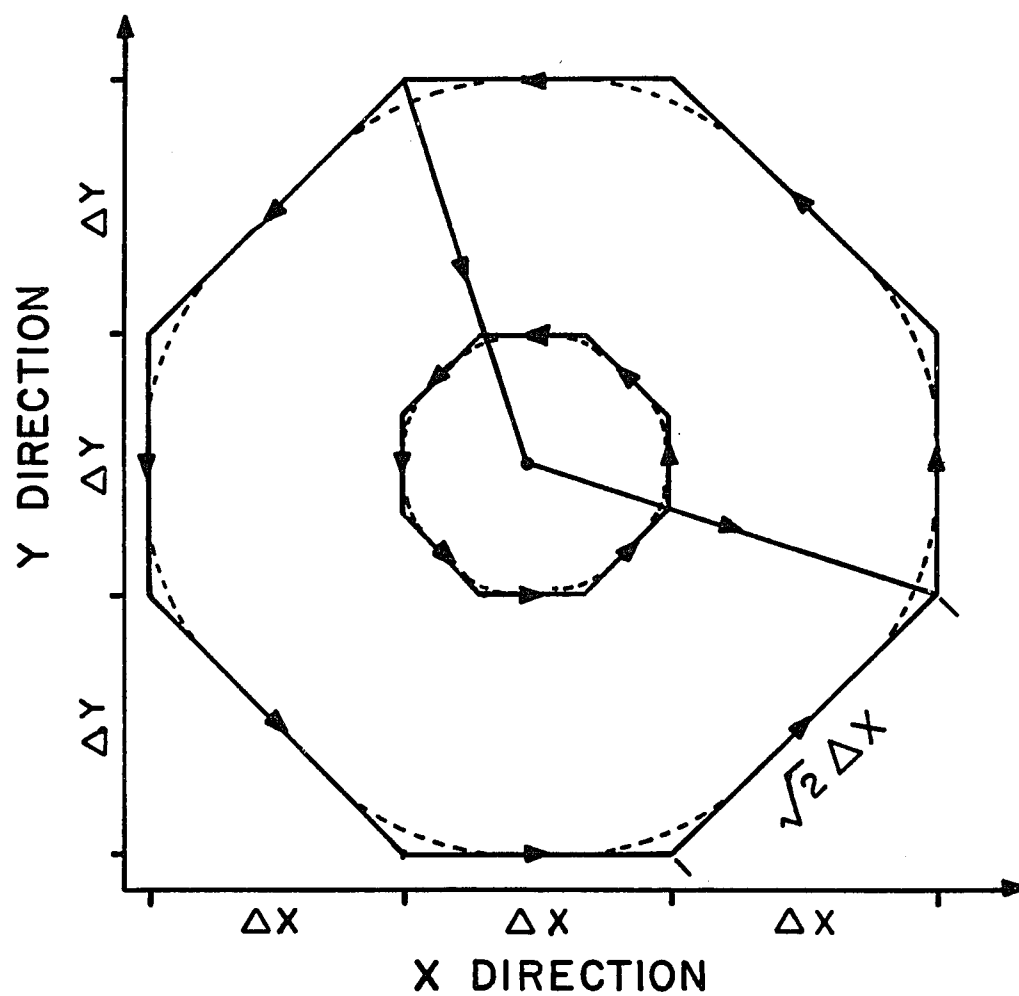


Figure 7. HP Octagonal Scanning Pattern

Secondly, the corners are slightly rounded (dashed lines in Figure 7) because as the scan gets to within approximately two millimeters of an upcoming corner, movement begins toward the following corner. This is to prevent the occurrence of any pauses during the therapeutic scanning process, which could cause excessively hot areas.

Refer to the program flowchart shown in Figure 8 to aid the following description. The software assumes scanning is to begin at the center of the octagon, and therefore measures these voltages. The operator inputs the desired size of the octagon, and all voltages which should appear at the corners of the octagon are calculated. The HP sequentially outputs these voltages to produce the octagon. This continues for the duration of treatment. If an internal scan is desired, it is so specified by the operator along with its size. The scan will then alternate from external octagon to internal octagon to external octagon, doing any number of cycles at each position. The octagonal pattern has performed well and continues to be used.

### 2.3.2 Apple IIe - Anaheim Indexers/Octoson® Interface Software

The major scanning patterns are an octagon (Figure 9) and a raster-filled circle (Figure 10). The octagonal pattern is different than the previous description in the following ways. First, the operator can specify equal length X and Y dimensions or unequal length X and Y dimensions. That is, the pattern can become rectangular in shape, with straight-line segments used to cut the corners of the

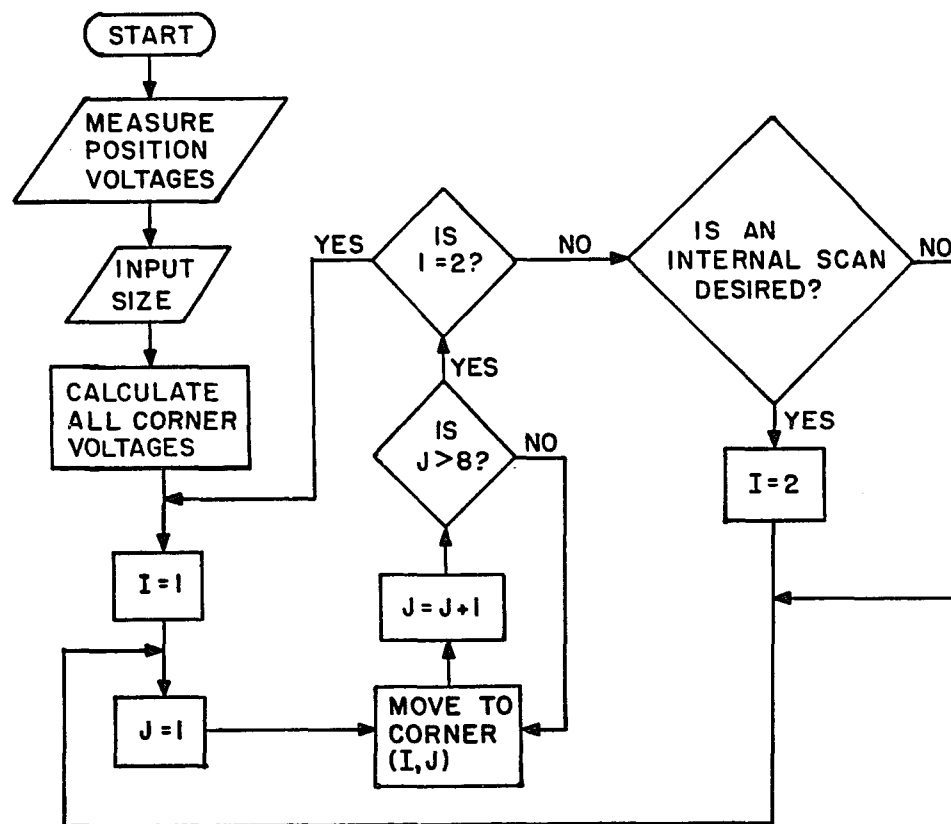


Figure 8. Simplified Program Flowchart for the HP Octagonal Scanning Pattern

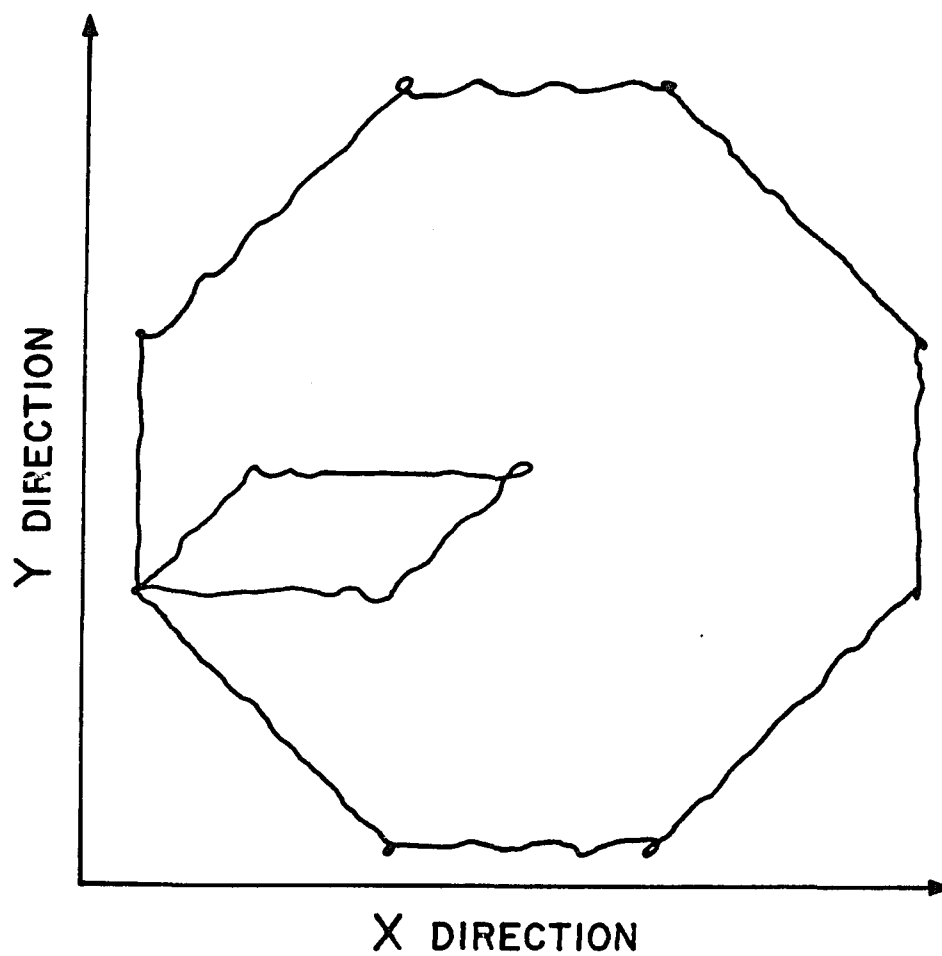


Figure 9. Copy of an Actual Trace of the Apple IIe - Anaheim Indexers Octagonal Scanning Pattern

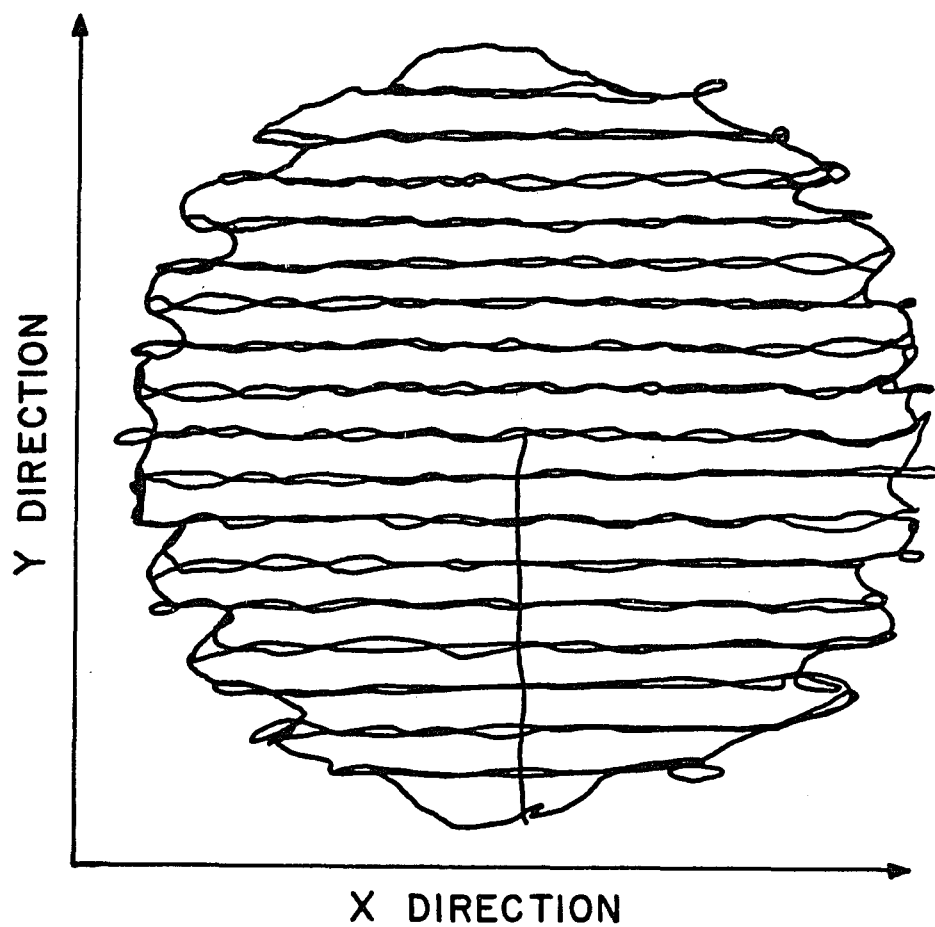


Figure 10. Copy of an Actual Trace of the Apple IIe - Anaheim Indexers Raster-Filled Circular Scanning Pattern

short sides (see Figure 11). Also, the corners are not rounded as they are with the HP octagonal pattern. This is because the Anaheim Indexers know the instant motion ends, and in a matter of microseconds start the next move. The HP, on the other hand, is responsible for monitoring when a move is nearing completion. Therefore, a pause is noticed if a move is allowed to make it all the way to its programmed end. The raster-filled circle provides another method of scanning the interior of a tissue volume as compared with interior concentric octagons. The flowcharts for the octagon and raster-filled circle are given in Figures 12 and 13, respectively, and will aid the following program descriptions.

The software for the octagon assumes motion is to begin at the center of the octagon. The operator specifies the number of concentric octagons to be scanned, along with the size of each and the number of cycles to scan for each size. The number of motor steps between each corner of the octagon is calculated. The operator inputs the desired speed of travel to be used. The scanning of concentric octagons is performed until instructed to stop. The program ensures a constant speed of travel even during diagonal-line segments by reducing the speed in both the X and Y directions by the square root of two. During all straight-line segments the program determines if the gantry is at its proper location via the safety potentiometers described previously in section 2.2.3. The octagonal pattern can also be performed at different Z positions, thereby producing an octagon-shaped cylinder.

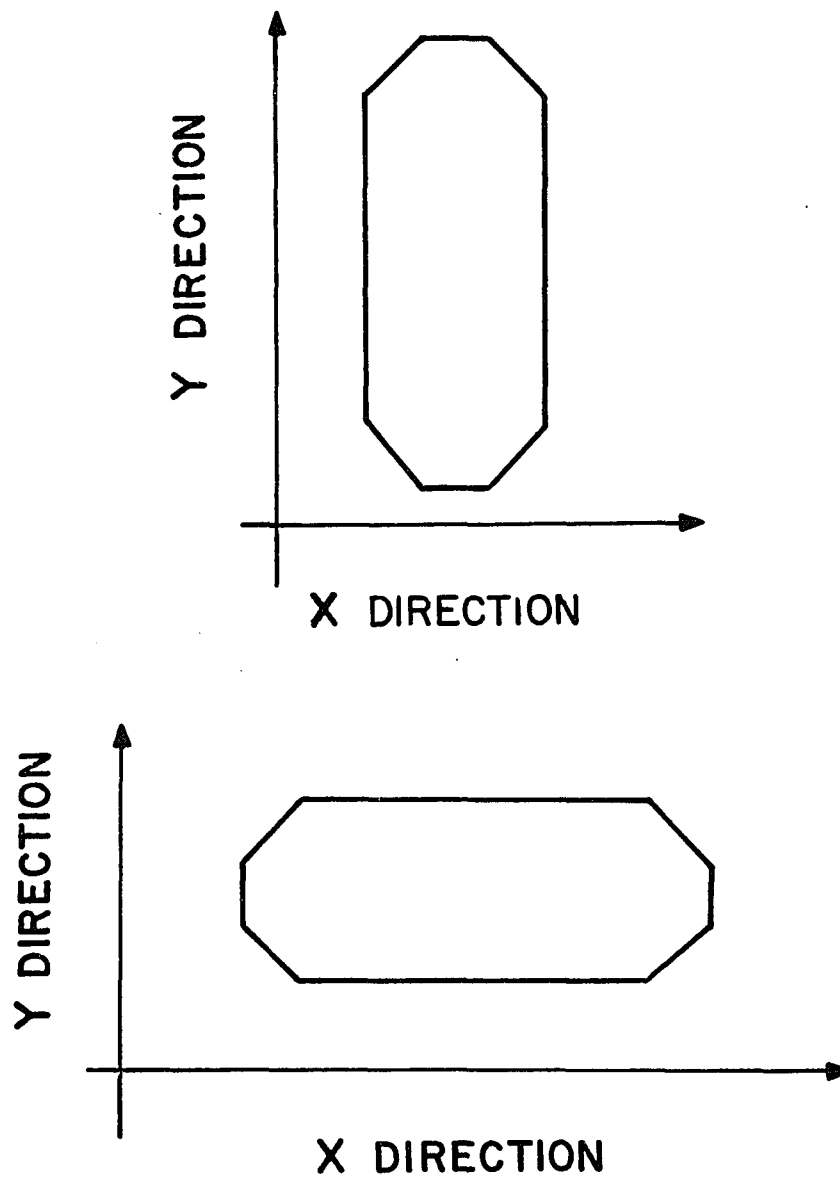


Figure 11. Exemplary Sketches of the Apple IIe - Anaheim Indexers Elongated Octagonal Scanning Pattern

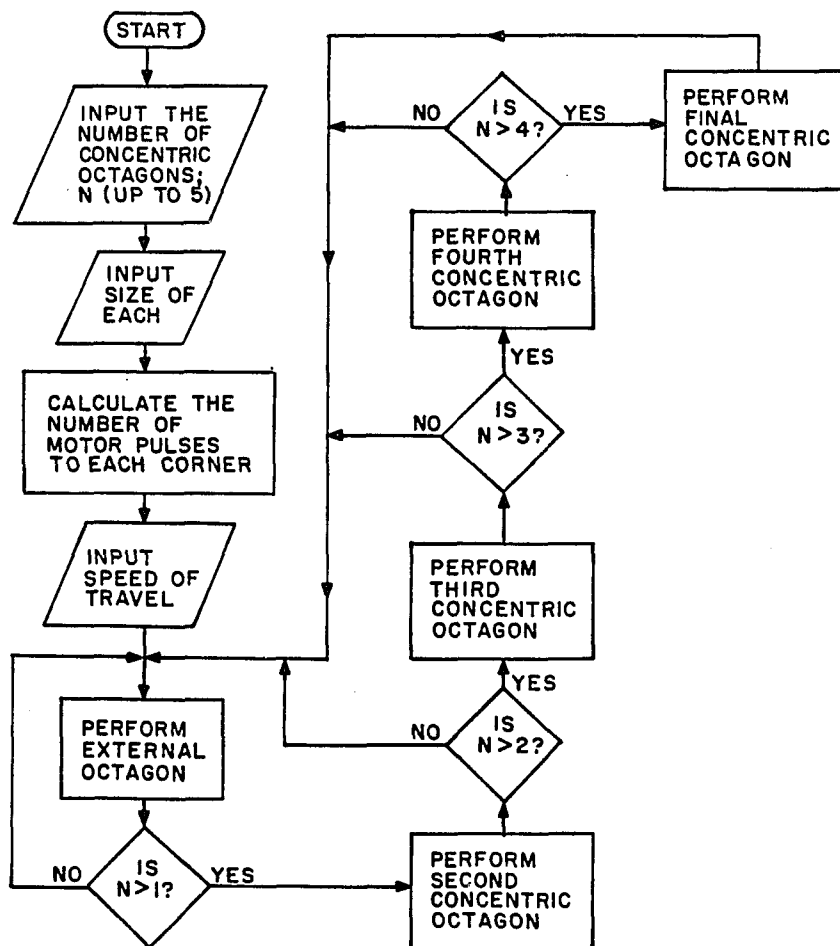


Figure 12. Simplified Program Flowchart for the Apple IIe - Anaheim Indexers Octagonal Scanning Pattern



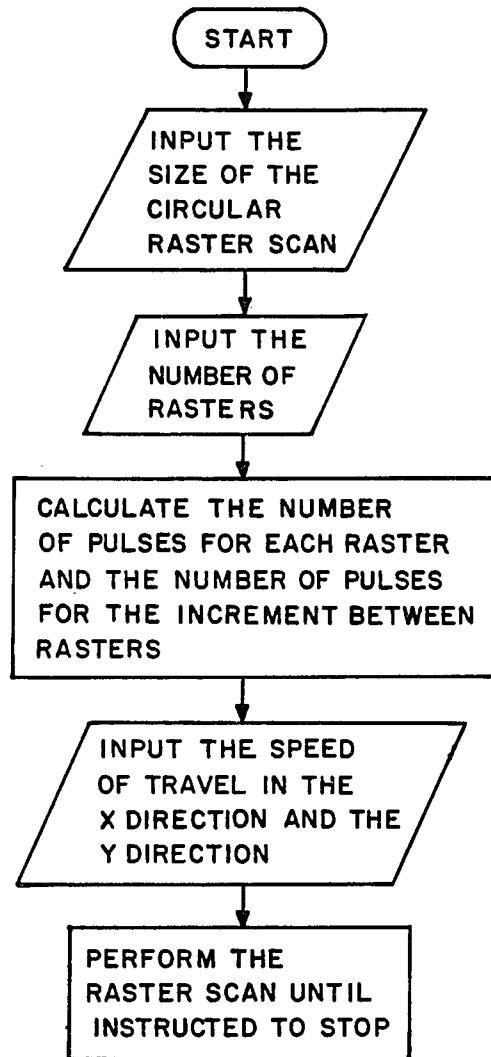


Figure 13. Simplified Program Flowchart for the Apple IIe - Anaheim Indexers Raster-Filled Circular Scanning Pattern

The software for the raster-filled circle also assumes scanning begins at the center of the circle. The operator inputs the diameter of the circle, the number of rasters desired, and the speed of travel for the X and Y directions. The X direction is used as the direction of primary motion because, as will be seen Chapter 3, it provides a higher speed. The Y direction, on the other hand, is used for incremental motion between rasters as speed in this direction is restricted. The number of motor steps needed for each raster and for the increment between rasters are calculated. The scan is performed until the operator instructs it to stop. Again, the feedback potentiometers are utilized to verify gantry position for safety purposes. The raster-filled circular pattern can also be performed at different Z positions, thereby producing a cylindrical pattern.

The geometric patterns which can be scanned using this interface are unlimited. As a matter of fact, a program has been developed which will scan any three dimensional pattern. All it requires is an array of X, Y, and Z coordinates which define the pattern, with the remainder of the program description similar to the previous two. After constructing a three-dimensional volume from a series of two-dimensional cross sectional scans from the Octoson®, the HP computer determines an array of X, Y, and Z coordinates which define the points to scan. This array is then available for use with the scanning program. The program converts the values in the array into the number of motor steps between each point. The therapeutic focus is scanned

successively from point to point, and continues until instructed to stop. This program has yet to be used for experiments.

From the hardware and software descriptions of each movement system interface, i.e., HP/Octoson® interface and Apple IIe - Anaheim Indexers/Octoson® interface, it can be concluded that the latter provides the best scanning versatility. Not only can the operator control the speed of travel, but rather he can control all those parameters which utilize the indexers full versatility (see Appendix A for a complete list of these parameters). For this reason, the Apple IIe - Anaheim Indexers/Octoson® interface is used exclusively for therapeutic scanning. Table 8 is a list of programs available for use with this interface, including a short description of each. The program names are kept long for no other reason than being thoroughly descriptive. Keep in mind that, for all programs, speed, acceleration, deceleration, and distance to move (or size) are all under operator control. Also, when each program is run the first page gives a more detailed description of what the program does and how to use it.

Table 8. Program Names and Descriptions

Program Name	Description
Test Programs	
XYTEST ZTEST RTEST TTEST SIMPLE A/D	These programs are used to test the system. It was by these programs that the data in Chapter 3 on maximum speeds, overshoot, calibrations, and reliability were obtained.
Treatment Programs (Two-Dimensional)	
XYOCTAGON5POTS	This program scans concentric octagons in the X Y plane and monitors gantry position for safety purposes.
XZOCTAGON5POTS	Same as previous, but in the X Z plane.
CIRCLERASTERPOTS	This program performs the raster-filled circular scan in the X Y plane and monitors gantry position for safety purposes.
(Three-Dimensional)	
CYLINDERXYOCTAGON5POTS	This program performs concentric octagons at different Z positions and monitors gantry position for safety purposes.
CYLINDERRASTERPOTS	This program performs the raster-filled circular pattern at different Z positions and monitors gantry position for safety purposes.
GENERAL	This program scans any three-dimensional volume given an array of X, Y, and Z coordinates which define the points to scan.

## CHAPTER 3

### SYSTEM CALIBRATIONS AND RELIABILITY TESTS

This chapter describes the calibrations and tests done to obtain comprehensive knowledge of the system's operation, and presents the results. The calibrations performed (for each direction of travel) include the amount of overshoot during scanning as a function of the indexer parameters, the maximum speeds attainable, and the distance traveled per motor step. Reliability tests performed consisted of scanning a given pattern for several hours at a time to determine how accurately the pattern repeated itself. The results are presented in graphical form.

#### 3.1 Octoson Positioning Repeatability

Inherent to the Octoson® are idiosyncrasies which cause the system to become inoperable (see Appendix B for a description of these). The only ways to recover from these failures are either a power off/on sequence or an initialization. A power off/on sequence will reset the total system, whereas an initialization resets only the gantry positioning circuitry.

Due to the occurrence of these idiosyncrasies, studies were done to determine how accurately the gantry returned to its previous position after a power off/on sequence and after an initialization. The tests were performed in the following manner.

A pointer was attached to the transducer gantry in a manner which simulates the ultrasonic focus. Two steel rulers (with millimeters as their smallest divisions) were fixed to the outside of the tank above the opening to simulate a patient's skin line.

For the power off/on study, the system was powered on and the transducer gantry moved to a random position via the positioning potentiometers on the front panel of the Octoson® console. This position was recorded. A power off/on sequence was then done, and the difference between the new position and the previous position was measured. The trial was performed 25 times, with the results shown in Table 9.

For the reinitialization study, the system was powered on, and remained on. The system was initialized and the transducer gantry moved to a random position via the positioning potentiometers. This position was recorded. A reinitialization was then done, and the difference between the new position and the previous position was measured. The results for 25 trials appear in Table 10.

The same general procedure was used to obtain the data in Tables 11 and 12. For Table 11, the system was powered on and the gantry was moved to a random position via the positioning potentiometers. This position was recorded. An initialization was then done, and the difference between the new position and the previous position was measured. Note that this is the first initialization immediately following a power on. The trial was repeated 25 times.

Table 9. Displacement (in mm) From Previous  
Position due to Power Off/On Sequences

Trial	Direction		
	X	Y	Z
1	0.00	0.00	0.00
2	0.00	0.00	0.00
3	0.00	0.00	0.00
4	0.00	0.00	0.00
5	0.00	0.00	0.00
6	0.00	0.00	+1.00
7	0.00	0.00	0.00
8	0.00	0.00	0.00
9	0.00	0.00	0.00
10	0.00	0.00	0.00
11	0.00	0.00	0.00
12	0.00	0.00	0.00
13	0.00	0.00	0.00
14	0.00	0.00	0.00
15	0.00	0.00	-1.00
16	0.00	0.00	0.00
17	0.00	0.00	0.00
18	0.00	0.00	0.00
19	0.00	0.00	0.00
20	0.00	0.00	0.00
21	0.00	0.00	0.00
22	0.00	0.00	0.00
23	0.00	0.00	0.00
24	0.00	0.00	0.00
25	0.00	0.00	0.00

Table 10. Displacement (in mm) From Previous  
Position due to Repeated Initializations

Trial	Direction		
	X	Y	Z
1	0.00	+0.25	0.00
2	0.00	-0.25	-1.00
3	0.00	0.00	+1.00
4	0.00	0.00	0.00
5	0.00	0.00	+1.00
6	0.00	0.00	-1.00
7	0.00	0.00	0.00
8	0.00	0.00	+1.00
9	0.00	0.00	-1.00
10	0.00	0.00	0.00
11	0.00	0.00	-1.00
12	0.00	0.00	+0.50
13	0.00	0.00	-0.50
14	0.00	0.00	0.00
15	0.00	0.00	0.00
16	0.00	0.00	+1.00
17	0.00	0.00	-1.00
18	0.00	0.00	-0.50
19	0.00	0.00	+0.50
20	0.00	0.00	0.00
21	0.00	-0.25	0.00
22	0.00	0.00	-1.00
23	0.00	+0.25	+0.50
24	0.00	0.00	0.00
25	0.00	0.00	+0.50



Table 11. Displacement (in mm) From Previous Position  
due to Initialization Following Power On

Trial	Direction		
	X	Y	Z
1	0.00	+0.25	-3.00
2	0.00	+0.25	-3.00
3	0.00	0.00	-3.00
4	0.00	0.00	-3.00
5	0.00	0.00	-3.00
6	0.00	0.00	-3.00
7	0.00	0.00	-3.00
8	0.00	0.00	-3.00
9	0.00	0.00	-3.00
10	0.00	0.00	-3.00
11	0.00	0.00	-2.00
12	0.00	0.00	-3.00
13	0.00	0.00	-3.00
14	0.00	0.00	-3.00
15	0.00	0.00	-3.00
16	0.00	0.00	-3.00
17	0.00	0.00	-2.00
18	0.00	0.00	-3.00
19	0.00	0.00	-2.00
20	0.00	0.00	-2.00
21	0.00	0.00	-2.00
22	0.00	0.00	-2.00
23	0.00	0.00	-3.00
24	0.00	0.00	-2.00
25	0.00	0.00	-2.00

Table 12. Displacement (in mm) From Previous Position  
due to Power Off/On Following Initialization

Trial	Direction		
	X	Y	Z
1	0.00	0.00	+3.00
2	0.00	0.00	+3.00
3	0.00	0.00	+3.00
4	0.00	0.00	+2.00
5	0.00	0.00	+3.00
6	0.00	0.00	+2.00
7	0.00	0.00	+3.00
8	0.00	0.00	+3.00
9	0.00	+0.25	+2.00
10	0.00	0.00	+2.00
11	0.00	0.00	+3.00
12	0.00	0.00	+3.00
13	0.00	0.00	+3.00
14	0.00	+0.25	+3.00
15	0.00	0.00	+3.00
16	0.00	0.00	+3.00
17	0.00	0.00	+3.00
18	0.00	0.00	+2.00
19	0.00	0.00	+2.00
20	0.00	0.00	+3.00
21	0.00	0.00	+3.00
22	0.00	0.00	+3.00
23	0.00	0.00	+2.00
24	0.00	0.00	+2.00
25	0.00	0.00	+2.00

For Table 12, the system was powered on and initialized. The gantry was moved to a random position via the position potentiometers, and this position recorded. The system was then powered off and on, and the difference between the new position and the previous position was measured. Note that this is a power off/on sequence immediately following an initialization.

The results in Tables 9 and 10 indicate that a power off/on sequence returns the transducer gantry to its exact previous position more often than an initialization. A power off/on sequence may not always be feasible, however, and the largest difference of  $\pm 1$  millimeter for an initialization is acceptable. Tables 11 and 12 indicate that the operator should be consistent in the selection of corrective action. Using either a power off/on sequence or an initialization, rather than alternating between them, will allow the least possible difference between the new and previous positions.

### 3.2 Indexer Calibrations

This study was performed to determine the distance traveled in each direction given a specified number of pulses (motor steps) from the respective indexer. Again, the pointer mounted on the transducer gantry and the measuring instruments served the purpose of indicating displacement.

The indexers were instructed by the Apple IIe to drive the motors a given number of steps, and the corresponding distances were measured. From this the number of motor steps per millimeter or

degree for X, Y, and Z or R and T, respectively, were calculated. The results are presented in Table 13, and correspond with the "divide by" circuitry of the Octoson®, which is used for displaying distances on the video screen. These data will not change unless hardware modifications particular to movement mechanics are done, e.g., changing gear sizes or using other than eight phase stepper motors.

### 3.3 Movement System Overshoot

Due to the large mass of the transducer gantry, there exists mechanical overshoot during scanning. Because the ultrasonic focus is approximately 35 centimeters above the gantry, its overshoot is further accentuated. Overshoot is not necessarily bad, however, so long as it is taken into account when entering the desired size to scan. In order to account for overshoot, it needed to be studied as functions of those indexer parameters which define a move.

As described in section 2.2.2, the indexers provide the user good scanning versatility. Briefly, the user has control over the base rate, maximum rate, acceleration, deceleration, and size parameters to be used during a move. It was felt that overshoot may be a function of any or all of these parameters, and thus each was investigated. When studying overshoot as a function of base rate, acceleration and deceleration were set to zero thereby causing the entire move to be made at the base rate. (See Appendix A for more information on indexer operation.) When studying overshoot as a

Table 13. Indexer Calibration Data

Direction	Pulses (Motor Steps) Per Millimeter of Degree	Incremental Resolution
X	16 pulses/mm	1/16 mm
Y	34 pulses/mm	1/34 mm
Z	70 pulses/mm	1/70 mm
R	34 pulses/deg	1/34 deg
T	70 pulses/deg	1/70 deg

function of maximum rate, acceleration and deceleration, the base rate was chosen such that it contributed no overshoot.

For all the studies, a drawing instrument was fixed to the transducer gantry in a manner which simulates the ultrasonic focus. An apparatus was set up such that an actual trace of the movement was obtained on paper. The distance of the trace on the paper was measured and subtracted from the programmed movement distance. The result is the amount of overshoot.

The data will be presented sequentially for each of the five directions (X, Y, Z, R, and Y), along with a discussion for each. Graphical presentation will be used.

### 3.3.1 X Direction Overshoot

Figure 14 presents X overshoot as a function of base rate and Z position - since it was felt that more overshoot may be associated with the gantry suspended higher. The results indicate that X overshoot is a function of both base rate and Z position. This is reasonable because trying to instantly stop the same mass traveling at increasing speeds is essentially trying to convert increasing kinetic energy into energy of another form in the same time. Of course, this is not possible and is the principle being observed.

The increased overshoot with increasing Z can be explained with reference to pendulum theory. Suppose a mass suspended on a string is set in motion. If one stops the mass by grabbing the

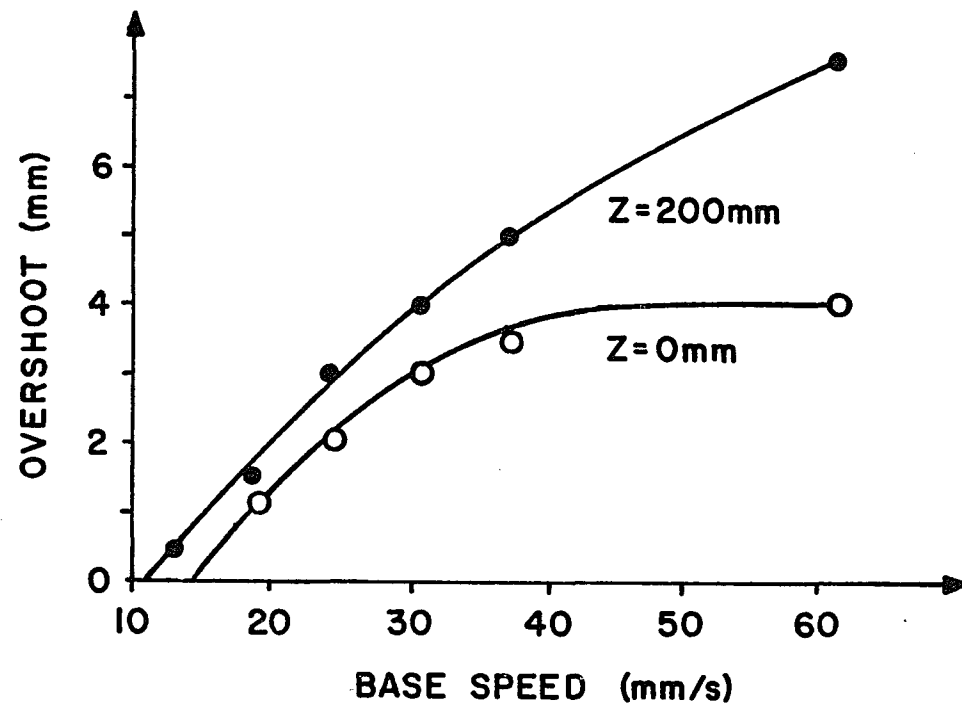


Figure 14. X Director Overshoot as a Function of Base Speed and Z Position  
Parameters: Acceleration =  $\emptyset$ , Deceleration =  $\emptyset$ , Distance Traveled = 100 mm

string near the mass, the length of the arc displaced is less than if the string is grabbed farther away from the mass. The overshoot data does not exactly follow pendulum principles for the simple reason that the movement system is attached at four or more places, rather than at one point as for a pendulum. However, the basic theory remains valid.

Figure 15 presents X overshoot as functions of the maximum speed of travel, the acceleration characteristic used, and the deceleration characteristic used, and Z position. The results indicate that X overshoot is a strong function of the maximum speed of travel and of the deceleration characteristic used, but not a strong function of the acceleration characteristic used. Again, the pendulum explanation is valid for overshoot due to deceleration, but the reason for overshoot due to acceleration requires a different explanation.

Because the ultrasonic focus is approximately 35 centimeters above the transducer gantry, the gantry acts like the fulcrum of a lever. Therefore, as motion begins in one direction, the focus is displaced slightly in the opposite direction before proceeding in the direction of motion.

The Z position has little affect when using any amount of acceleration and deceleration. This is explained by the fact that even the fastest acceleration and deceleration correspond with movements starting and ending at speeds less than a base speed of 15mm/s, where overshoot is not a strong function of Z position (this is illustrated in Figure 14).



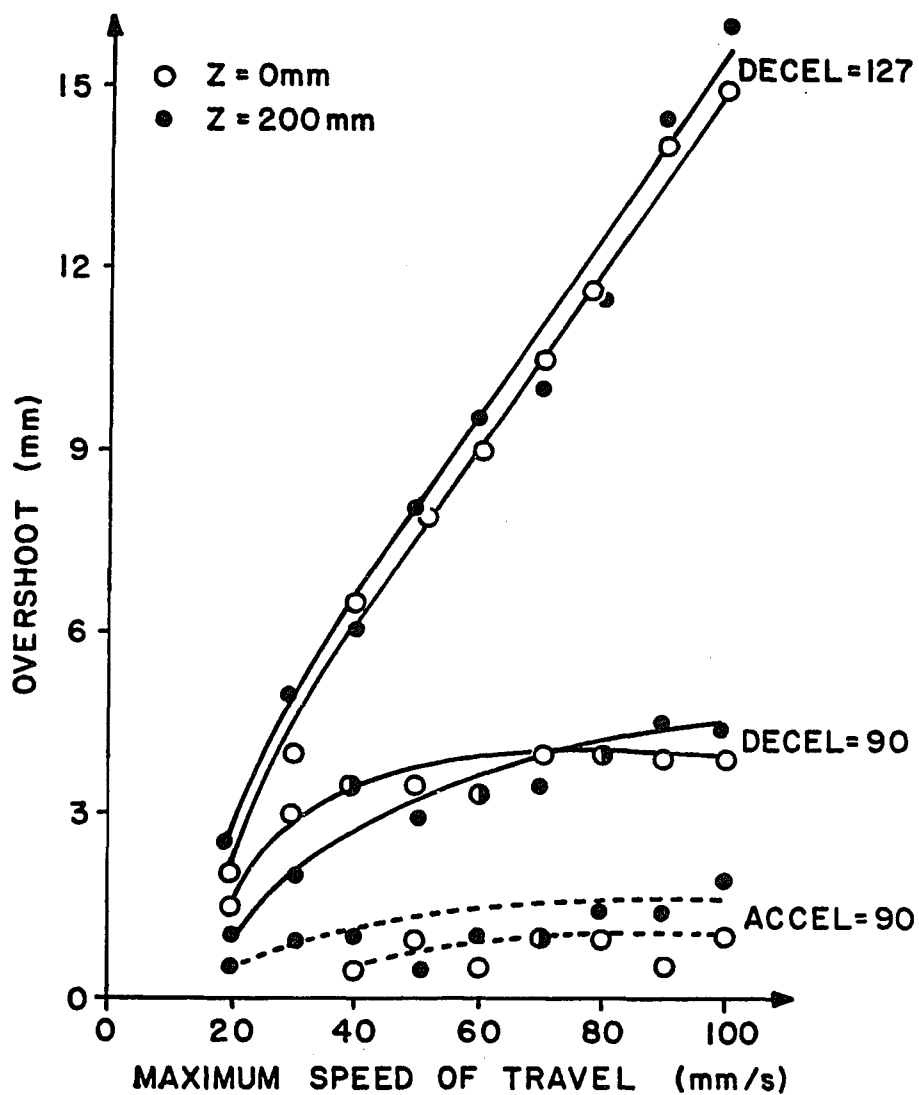


Figure 15. X Direction Overshoot as a Function of Maximum Speed, Acceleration, Deceleration, and Z Position  
 Parameters: Base Speed = 7.5 mm/s,  
 Distance Traveled = 100 mm  
 Horizontal axis corresponds with Acceleration = 0,  
 Deceleration = 1

### 3.3.2 Y Direction Overshoot

Figure 16 presents the results of Y overshoot as a function of base rate and Figure 17 presents the results of Y overshoot as a function of maximum rate, acceleration, deceleration, and Z position. The graphs indicate that overshoot in the Y direction is less significant than overshoot in the X direction. This is for two reasons; 1) the Y direction has a more restricted range of speeds than does the X direction, and 2) the gantry is more securely fixed in the Y direction than in the X direction, i.e., different tracks and bearings provide less vibrations and freeplay.

As with the X direction, the graphs for Y overshoot indicate that overshoot is a stronger function of deceleration than it is of acceleration. Because both directions are horizontal translations, the explanation for this is as it was for X overshoot. Also, the reasons for Y overshoot being a weak function of Z position are as the explanation for X overshoot.

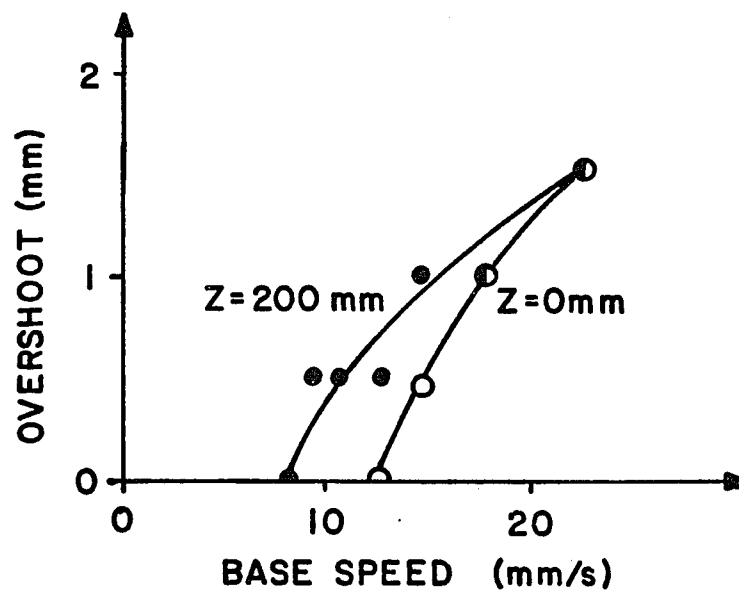


Figure 16. Y Direction Overshoot as a Function of Base Speed and Z Position  
Parameters: Accel = 0, Decel = 0,  
Distance Traveled = 100 mm

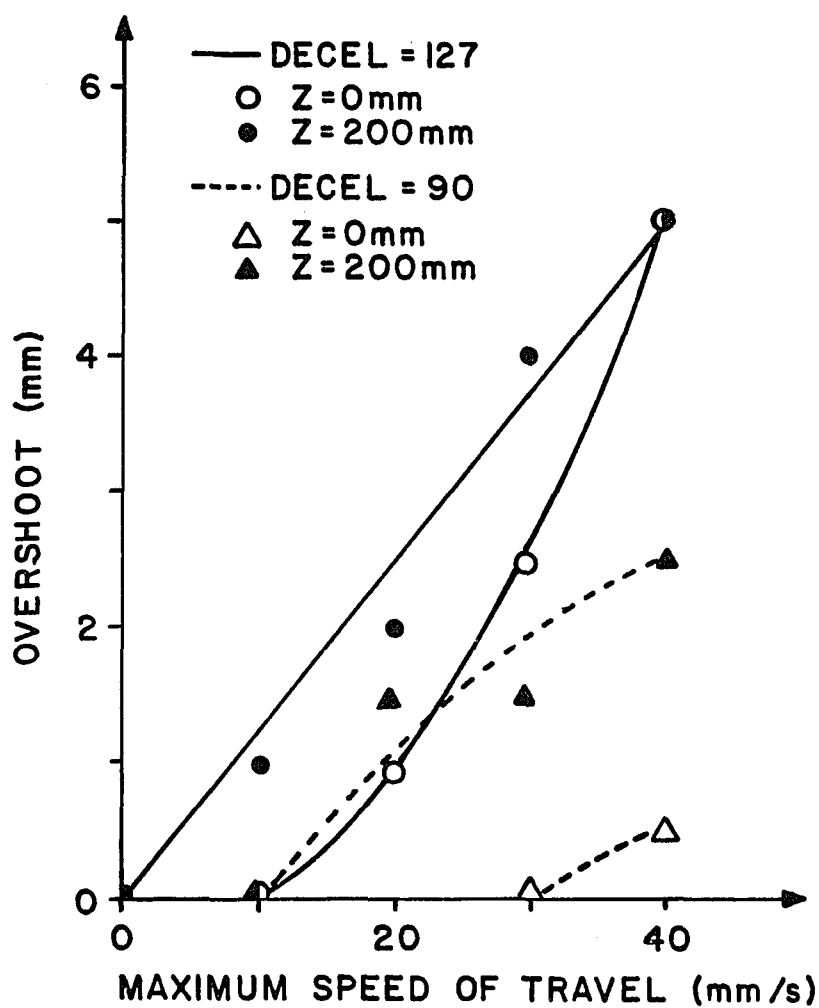


Figure 17. Y Direction Overshoot as a Function of Maximum Speed, Acceleration, Deceleration, and Z Position  
 Parameters: Base Speed = 3.5 mm/s  
 Distance Traveled = 100 mm  
 Horizontal Axis Corresponds with Accel = 0-127, Decel = 1.

### 3.3.3 Z Direction Overshoot

Figures 18 and 19 present the results of Z overshoot as functions of base rate, maximum rate, acceleration, and deceleration. Although the results for Z overshoot are similar to those for X and Y overshoot, subtle differences do exist. Overshoot in the Z direction remains a function of base rate, maximum rate, and deceleration, however it is not a function of acceleration at all. The reason for this is that no fulcrum and lever action exists in the Z direction, i.e., the line of movement is directly through the center of the gantry. One other interesting note is that overshoot in the Z direction occurs exclusively following a downward move. That is, no overshoot occurs at the end of an upward move. The only explanation for this is gravity; it aids the upward stop and hinders the downward stop.

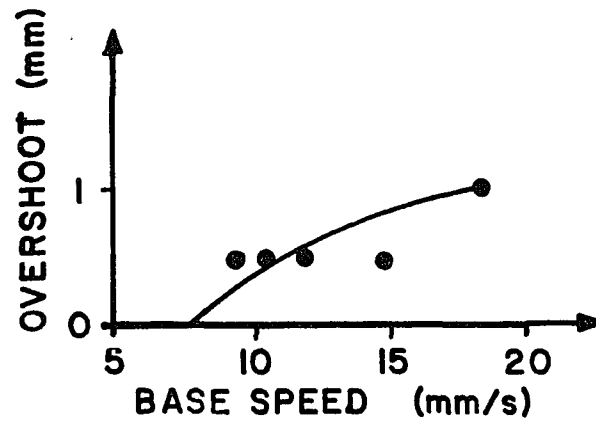


Figure 18. Z Direction Overshoot as a Function of Base Speed  
Parameters: Acceleration =  $\emptyset$ , Deceleration =  $\emptyset$ , Distance Traveled = 100 mm.

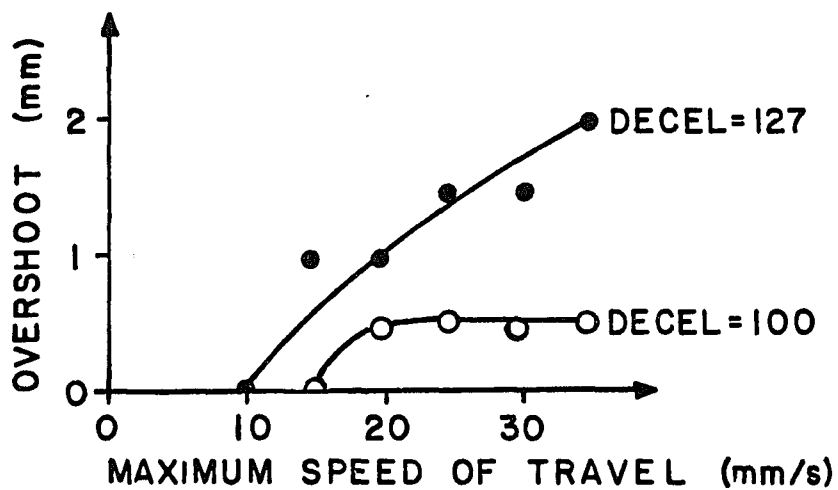


Figure 19. Z Direction Overshoot as a Function of Maximum Speed, Acceleration and Deceleration  
Parameters: Base Speed = 1.8 mm/s  
Distance Traveled = 100 mm  
Horizontal Axis Corresponds with Accel = 0-127, Decel = 1.

#### 3.3.4 R Direction Overshoot

It is unnecessary to present graphically the results of R overshoot as functions of base rate, maximum rate, acceleration, and deceleration as the data indicate that no overshoot occurs along the arc of rotation for any values of indexer parameters. The study of R direction overshoot did reveal, however, that rotate is very sensitive to acceleration and deceleration with regard to loss of motor synchronization. Rotate has yet to receive much attention for therapeutic scanning, but this fact must be considered if utilization of rotate increases.

#### 3.3.5 T Direction Overshoot

Figures 20 and 21 present the results of T overshoot as a function of base rate, maximum rate, acceleration, and deceleration. The results indicate that tilt overshoot is a function of base rate, maximum rate, and deceleration, but not a function of acceleration. All overshoot for tilt is minimal because movement in this direction moves only the transducer assembly, the least amount of mass for any direction. In comparison, Z moves the transducer assembly and tilt movement mechanics, R moves the transducer assembly and Z and T movement mechanics, X moves the transducer assembly and R, Z, and T movement mechanics, and Y moves the transducer assembly and X, R, Z, and T movement mechanics. As with rotate, tilt has yet to receive much attention with regard to therapeutic scanning.



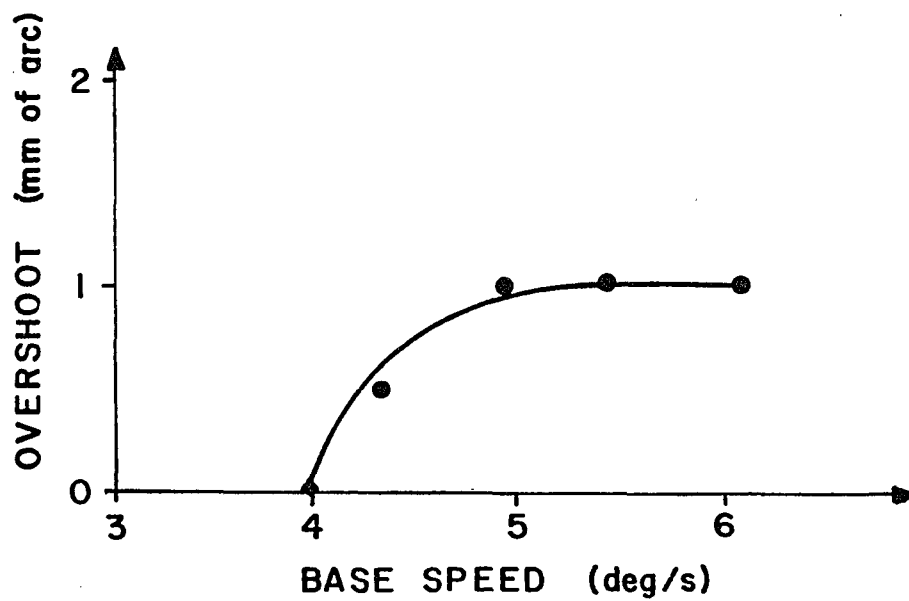


Figure 20. T Direction Overshoot as a Function of Base Speed  
Parameters: Acceleration =  $\emptyset$ , Deceleration =  $\emptyset$ ,  
Distance Traveled = 30 degrees

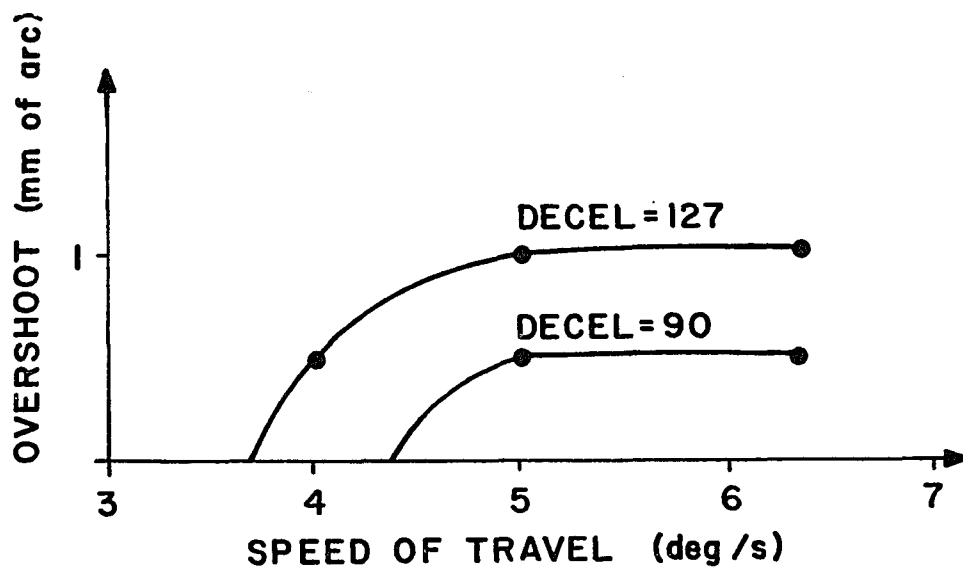


Figure 21. T Direction Overshoot as a Function of Maximum Speed, Acceleration and Deceleration  
Parameters: Base Rate = 1.8 degrees/s  
Distance Traveled = 30 degrees  
Horizontal Axis Corresponds with Accel = 0-127, Decel = 1.

### 3.3.6 Summary of Movement System Overshoot Studies

This section serves to briefly summarize the results of the overshoot studies. A note of significant importance is that the previous studies indicated that overshoot is not a function of size. That is, the previous studies were repeated for different distances to move and, so long as the maximum speeds specified were attained, the overshoot did not change. In all instances, if maximum speeds were not attained the overshoot was less than indicated. This must be considered when slow acceleration and deceleration are used. (The equations given in Appendix A allow one to determine if maximum speeds will be attained given acceleration, deceleration, and the number of motor steps to move.)

In general, the overshoot which occurs during therapeutic scanning is a function of indexer parameters which the operator has control over. This is desirable because one can account for the overshoot at the outset of a treatment. Typically, to perform scanning:

- 1) Select the indexer characteristics and speeds to be used during therapeutic scanning.
- 2) Refer to the graphs in this chapter to determine the overshoot due to the parameters in 1.
- 3) Compensate for the respective overshoot when entering the size scan to be performed.

The parameters used for experiments thus far have been acceleration 90 to 100, deceleration 90 to 100, and base rate 1.5 to 8.0 millimeters per second, for the following reasons. The above

acceleration and deceleration characteristics were selected because they allow maximum speeds to be attained with minimal overshoot for all sizes in all directions. Accelerations greater than 100 should be avoided as this, coupled with fast maximum speeds, will result in loss of motor synchronization. It is for this reason that no curves for accelerations greater than 90 were shown in Figure 15. The base rates were chosen low for no other reason than the belief that this would cause the least amount of wear to the stepper motors. The maximum speeds used during experiments have varied widely. Keep in mind, however, that all parameters are under operator control, and can be changed with minimal effort.

### 3.4 Maximum Speeds Attainable

The purpose of this study was to determine the upper limit of speed available for each direction. The drawing instrument attached to the gantry produced traces of distances traveled, thus providing visual data of loss of motor synchronization. Loss of motor synchronization is also audible, i.e., the stepper motors make distinct grinding noises as they slip.

This study consisted of driving each motor a known distance at a given speed, and listening for unusual noises while obtaining the actual trace. The distance of the trace was measured and if the value was less than the programmed distance, the motor lost synchronization because it was driven too fast. If the motor lost synchronization at a given speed, the trial was run again at a reduced speed. On the other hand, if the motor did not lose synchronization, the

trial was run again at an increased speed. This process of elimination continued until the maximum attainable speeds (Table 14) were obtained. It should be noted that these data are for loss of synchronization which is instantly noticed, i.e., after one move.

Long term studies (one hour of scanning) were done to determine if any loss of synchronization which is not instantly noticed was occurring over time. The same procedure as above was used, with the exception that scanning continued for an hour instead of stopping after one move. The results did indicate a slow drift with time in all directions at the speeds in Table 14. The process of elimination was repeated for long term scans until speeds at which no loss of synchronization occurs were obtained. The speeds are given in Table 15.

The maximum speeds are very dependent on movement system mechanics, and, as a matter of fact, have been the first indicators that certain mechanical components (i.e., bearings) needed replacing. That is, if one notices any reductions in the maximum speeds attainable for a given direction, prepare to perform system maintenance on that direction.

It should be noted that if the temperature of the motor rises above the manufacturer's specifications (90°C), loss of motor synchronization occurs at very slow stepping rates. This is particularly important because the motors are being driven at faster than recommended rates. Excess temperatures have not been a problem for the X, Z, R, and T motors as they are submersed in the temperature controlled water bath. However, because the Y motor is external to the tank, a fan was mounted nearby to cool it.

Table 14. Maximum Speeds Attainable Before Loss of Motor Synchronization is Instantly Noticed

Direction	Distance Traveled	Base Speed	Maximum Speed
X	200 mm	7.5 mm/s	108 mm/s
Y	200 mm	3.5 mm/s	37 mm/s
Z	200 mm	1.8 mm/s	39 mm/s
R	180 deg	3.5 deg/s	30 deg/s
T	36 deg	1.8 deg/s	6 deg/s

Parameters: Acceleration = 90, Deceleration = 90, and Factor = 10 (Factor = 6 for Z).

Table 15. Maximum Speeds Attainable Before Loss of Motor Synchronization is Noticed With Time

Direction	Distance Traveled	Base Speed	Maximum Speed
X	200 mm	7.5 mm/s	102 mm/s
Y	200 mm	3.5 mm/s	32 mm/s
Z	200 mm	1.8 mm/s	32 mm/s
R	180 deg	3.5 deg/s	23 deg/s
T	36 deg	1.8 deg/s	5 deg/s

Parameters: Acceleration = 90, Deceleration = 90, and Factor = 10 (Factor = 6 for Z).

### 3.5 Reliability Tests

The reliability of the system was tested by performing a given scanning pattern for one hour for each direction. The drawing instrument attached to the gantry provided the resulting traces. The results indicated that so long as less than maximum speeds are used during scanning, the patterns exactly repeated themselves. Examples of this were shown previously in Figures 9 and 10 of section 2.3.2. Figure 9 is an enlarged copy of an actual trace of the octagon pattern which was scanned for one hour at a constant speed of 30 millimeters per second. The number of repeated cycles during this time was approximately 330. Figure 10 is an enlarged copy of an actual trace of the raster-filled circle pattern, also scanned for one hour. The speed of travel was 70 millimeters per second in the X direction and 30 millimeters per second in the Y direction. These speeds allowed approximately 135 cycles to be repeated. In all instances, the trace remains no thicker than the tip of the drawing instrument, therefore indicating the patterns exactly repeat. Even the mechanical overshoot and damping exactly repeat.

### 3.6 Safety Potentiometer Calibration

As discussed in section 2.2.3, potentiometers were mounted inside the tank in the X, Y, and Z directions to provide position feedback for safety purposes. The calibration of the potentiometers was as follows.

The voltage across the potentiometers is 10 volts (regulated). The potentiometers are monitored by the Apple IIe via its 12 bit A/D



interface. A 12 bit A/D and a 10 volt range provide a resolution of 2.44 (10/4096) millivolts. The output of the A/D is a number in the range 0-4096 and, instead of converting it to voltage, this number was used as is.

The calibration of the potentiometers consisted of moving the gantry through its X, Y, and Z limits in 10 millimeter increments and recording the output of the A/D at each point. The data are given in Tables 16-18 for X, Y, and Z respectively. These data are dimensionless, but can be converted to millivolts by multiplying by 2.44. This is unnecessary, however, as the computer software uses the data as is.

The data indicates the presence of hysteresis when traveling in opposite directions along the same axis of motion. This is due to the freeplay which exists where the potentiometer gear mates with the movement system chains and tracks. The hysteresis is accounted for in the software, and has not been a problem. Table 19 summarizes the results of the calibration data.

The safety potentiometers were also studied for resistance changes with changing temperatures. The Octoson® water bath has a usable temperature range of 20 - 40°C. The potentiometers were monitored across this temperature range via the Apple IIe A/D interface. No changes what so ever were noticed in resistance across this range. This is confirmed by the manufacturer's specifications.

Table 16. X Direction Safety Potentiometer Calibration Data

Location From Center (in mm)	Direction of Motion				
	+X	-X	+X	-X	+X
-Limit		1732	1732	1730	1730
-120		1762	1746	1758	1741
-110		1840	1835	1850	1836
-100		1948	1924	1941	1922
- 90		2032	2019	2032	2020
- 80		2127	2109	2125	2106
- 70		2222	2204	2216	2206
- 60		2309	2289	2308	2290
- 50		2402	2383	2400	2388
- 40		2493	2479	2494	2474
- 30		2588	2568	2588	2570
- 20		2684	2658	2680	2660
- 10		2772	2753	2776	2752
0	2856	2866	2850	2866	2854
+ 10	2940	2960	2938	2960	
+ 20	3032	3052	3026	3048	
+ 30	3122	3144	3119	3138	
+ 40	3212	3230	3208	3228	
+ 50	3310	3326	3306	3326	
+ 60	3394	3412	3394	3410	
+ 70	3494	3504	3490	3504	
+ 80	3586	3598	3583	3598	
+ 90	3678	3697	3678	3696	
+100	3770	3788	3767	3788	
+110	3863	3878	3866	3876	
+120	3958	3972	3957	3966	
+130	4044	4058	4046	4058	
+Limit	4060	4060	4060	4060	

Note: This study began at center position traveling in the positive X direction and ended at center position traveling in the positive X direction, therefore completing two cycles of travel in both directions. Due to noise, all values are +/- 3.

Table 17. Y Direction Safety Potentiometer Calibration Data

Location From Center (in mm)	Direction of Motion				
	+Y	-Y	+Y	-Y	+Y
-Limit		20	20	20	20
-180		62	44	64	44
-170		182	173	188	176
-160		298	292	312	299
-150		442	416	444	418
-140		552	544	564	551
-130		696	680	700	678
-120		822	806	824	808
-110		950	936	952	946
-100		1076	1071	1082	1070
- 90		1206	1192	1216	1196
- 80		1336	1320	1340	1322
- 70		1470	1448	1468	1458
- 60		1592	1580	1595	1584
- 50		1722	1705	1720	1700
- 40		1845	1824	1846	1826
- 30		1978	1958	1982	1962
- 20		2100	2078	2102	2088
- 10		2218	2221	2232	2212
0	2340	2358	2342	2362	2340
+ 10	2472	2490	2470	2494	
+ 20	2598	2610	2592	2614	
+ 30	2724	2744	2722	2748	
+ 40	2850	2860	2852	2870	
+ 50	2980	2998	2978	3000	
+ 60	3098	3112	3097	3116	
+ 70	3226	3248	3228	3244	
+ 80	3362	3368	3352	3368	
+ 90	3490	3498	3486	3498	
+100	3616	3624	3608	3626	
+110	3749	3754	3740	3758	
+120	3868	3870	3865	3876	
+130	3988	4000	3988	4000	
+140	4094	4094	4094	4094	
+Limit	4094	4094	4094	4094	

Note: This study began at center position traveling in the positive Y direction and ended at center position traveling in the positive Y direction, therefore, completing two cycles of travel in both directions. Due to noise, all values are +/- 3.

Table 18. Z Direction Safety Potentiometer Calibration Data

Location From Zero Position (in mm)	Direction of Motion			
	+Z	-Z	+Z	-Z
-Limit	550	550	550	552
0	664	680	660	680
10	796	810	798	808
20	924	934	922	930
30	1048	1068	1048	1068
40	1180	1186	1178	1186
50	1300	1314	1302	1316
60	1428	1434	1428	1435
70	1556	1574	1558	1570
80	1682	1694	1681	1692
90	1814	1822	1813	1820
100	1942	1950	1940	1952
110	2072	2078	2070	2078
120	2192	2206	2192	2202
130	2324	2340	2325	2342
140	2448	2460	2448	2460
150	2580	2590	2584	2590
160	2699	2710	2702	2712
170	2834	2846	2830	2848
180	2956	2968	2956	2968
190	3082	3096	3080	3095
200	3218	3224	3218	3223
210	3340	3354	3344	3356
220	3464	3478	3466	3478
230	3596	3604	3598	3606
+Limit	3664	3664	3664	3664

Note: This study began at the lowest position for Z and, therefore, began travel in the increasing Z direction. Two complete cycles of travel in both directions were performed. Due to noise, all values are +/- 3.

Table 19. Safety Potentiometer Calibration Summary

Direction	Apple A/D Card Counts/mm	Converted to Volts/mm	Hysteresis (A/D Counts)
X	9.1	22.2 mV	15
Y	12.7	31.0 mV	12
Z	12.7	31.0 mV	13

## CHAPTER 4

### DISCUSSION

This thesis has presented a study of the mechanical movement system presently being used to investigate scanned, focussed, ultrasound hyperthermia. The calibrations, overshoot studies, and other tests performed on the movement system allow the operator to accurately predict how the system will operate given the necessary parameters to define a move.

In general, this investigation has shown the movement system to be both reliable and safe for scanning the ultrasonic transducers during hyperthermia treatments. The overshoot studies have shown that overshoot can be accounted for as it is a function of indexer parameters which the operator has control of. The reliability tests showed that so long as maximum speeds are not exceeded, scanning patterns exactly repeat. The safety potentiometers function to stop therapeutic scanning if the gantry fails to move in the manner prescribed by the program.

Besides all the tests described, in vivo experiments have been performed which have utilized the movement system extensively. (The reader is referred to Appendix C for a brief discussion of in vivo experimental results.) The system's feasibility as an effective hyperthermia device shall continue to be studied.

To pursue the feasibility of scanned, focussed ultrasound as a method to effectively induce hyperthermia for cancer treatment, further investigation is necessary. As investigation progresses, the movement system should continue to be improved upon.

Overshoot can be tolerated, however loss of motor synchronization is difficult to compensate for and is an area which should be investigated. The feedback potentiometers are presently monitoring loss of motor synchronization, with the software stopping treatment if it occurs. More sophisticated software (and possibly better monitoring, e.g., optical encoders) may allow corrective action in real time, thus allowing treatments to continue uninterrupted should drift occur.

As treatment protocols become established for particular cancers, another area which should be investigated is the therapeutic effectiveness of different scanning patterns. Rotate and tilt could be investigated as major axes of motion, and patterns utilizing all five degrees of freedom may have their niche.

In summary, a commercial ultrasound unit's mechanical movement system was modified to perform scanning during scanned, focussed, ultrasound hyperthermia. Extensive studies have been done on normal tissue. However, it hasn't been shown how effective the scanning will be on different cancer types. The next step in the investigation should be experimentation on actual cancer tissues.

## APPENDIX A

### INDEXER COMMANDS AND EXAMPLES

All indexer commands consist of a single letter, a letter and a number, or a letter and two numbers. All letters are upper case eight-bit ASCII coded characters with the most significant bit (MSB) set to zero. A delimiter must separate commands in a multi-command string, and in some cases must also separate bytes in multi-byte data. Valid delimiters are a comma, a space, or a carriage return. All invalid commands and data received by an indexer are ignored.

In the following command descriptions the data forms are defined as follows:

- a - - - one byte, range 1-6
- b - - - one byte, range 0-1
- c - - - one byte, A,B,C,D,F,I,J,L,M,N,O,P are valid
- dddd - - two bytes, range 0-65535
- ww - - - one byte, range 0-127
- xx - - - one byte, range 0-255
- yy - - - one byte, range 0-74
- zz - - - one byte, range 0-7

Also, the following form will be used to present command descriptions:  
Command (Mnemonic) - Definition.



### A.1 Command Descriptions

**AwW (Accel)** - Sets the rate of acceleration from base rate to maximum rate. If zero is specified, the move is made at the base rate.

**Bxx (Base)** - Sets the rate at which motions start and end.

**Dww (Decel)** - Sets the rate of deceleration from maximum rate to base rate. If zero is specified, the move terminates at the maximum rate.

**Eyy,yy (Enter)** - Allows a program to be entered for use in deferred execution mode. The first data byte indicates the buffer location to begin storing the program at, and the second data byte is the total number of buffer locations used by the program entered. The enter command itself uses no buffer locations, and one buffer location is used for each character entered, including delimiters.

**Fxx (Factor)** - Sets the rate division factor. This is actually a scaling factor for all rates. Entering zero will cause an error, and default is 1. A brief chart listing the range of stepping rates (in Hz) available for factor values from 1 to 20 is given below.

Factor	Rate #=0	Rate #=255
1	1111	20000
2	556	10000
3	370	6667
4	278	5000
5	222	4000
6	185	3333
7	159	2857
8	139	2500
9	124	2222
10	111	2000
11	101	1818
12	93	1667
13	85	1538
14	79	1429
15	74	1333
16	69	1250
17	65	1176
18	62	1111
19	58	1053
20	56	1000

G (Go) - Causes motion to begin after specifying the necessary parameters which define a move.

Hb (Home) - Find home. This command initiates a search for home in the direction last set.

Iz,yy (If) - If inputs = z, go to program buffer location yy, else go to next instruction. Used only in a stored program.

Jxx (Jog) - Sets the rate used for jogs, or short moves.

Lxx,yy (Loop) - Loop program a specified number of times. The first data byte entered specifies the number of times to perform the loop, and the second byte entered specifies the program buffer to loop to. No nesting of loops is permitted.

Mxx (Max) - Sets the maximum rate of movement. If the distance to move is big enough to accelerate and decelerate through the full speed range specified, then the remainder of the move is made at the maximum rate. However, if the distance is not large enough, then the indexer will accelerate only enough to allow complete deceleration back to base rate thus preventing the maximum rate from being attained. The following sketch depicts this pictorially.

Ndddd (Number) - Sets the relative distance to move.

Oz (Output) - Sets the trigger outputs to the binary pattern corresponding to the number specified.

Pdddd (Position) - Sets the next absolute position to go to.

Q (Quit) - Terminator for a stored program. It must be the last command sent when entering a program.

Ryy (Run) - Begin executing a stored program at specified buffer location yy.

S (Step) - Single step through a stored program.

Vc (Verify) - Verify previously entered data for a given parameter.

Wz (Wait) - Wait until the trigger input pattern corresponds to the binary pattern of the specified number z.

Xdddd (eXpend) - Sets a delay for the time specified.

Ya (Axis) - Selects the axis with which to communicate.

- Z (Zero) - Sets current position to absolute zero.
- + (CW) - Sets direction of shaft rotation to clockwise.
- (CCW) - Sets direction of shaft rotation to counter clockwise.

### A.2 Other Useful Indexer Information and Examples

The indexers can produce stepping rates from 5 to 20000 steps per second. The formula for computing the actual stepping rate is as follows:

$$\text{eq. 1) } \quad \text{steps/second} = \frac{f}{\text{Factor} (8100 - (30 \text{ Rate}))}$$

where  $f$  = crystal oscillator frequency (9 MHz)  
 Rate = Base or Max Rate # (0-255)  
 Factor = scaling factor (1-255).

This equation can be rearranged to solve for any of the unknowns. For example, suppose it is desired to start motion at 750 steps per second accelerate slowly to 10000 steps per second, and then decelerate slowly to complete the move. Determine Base Rate # and Max Rate #. From the table appearing with the factor command description one can see that a factor of 2 will be required. Rearranging the equation yields:

$$\text{eq. 2) } \quad \text{Rate \#} = 270 - \frac{300000}{(\text{steps/second}) (\text{Factor})}$$

Substituting Factor = 2 and the appropriate steps/second yields a Base Rate # of 70 and a Max Rate # of 255. To enter the above parameters and move 1000 steps with the first axis enter:

,Y1,A40,D40,B70,M255,N1000,G

Note that A and D were relative because specific characteristics were not specified, only slowly. The parameters can be given in any order because all calculations are done when the Go command is received. The formula to approximate the number of steps of acceleration is as follows:

eq. 3)

$$\# \text{ steps} = 10 + \frac{\text{Max} - \text{Base} - 2(\text{Accel}) + 3}{2} + \frac{(\text{Max} - \text{Base} - 2(\text{Accel}))^2}{8}$$

The approximate average rate during acceleration is:

eq. 4) Ave. Rate =  $0.67(\text{Max} - \text{Base} - 2(\text{Accel})) + \text{Base} + 2(\text{Accel})$

Decel may be used in place of Accel in the above equations to determine the number of steps of deceleration and average rate during deceleration.

By using equations 1 and 2 with a Factor of 10, Table A.1 was constructed. This table allows rapid determination of speed of travel from base rate of vice versa, which may prove useful when choosing parameters to be used for scanning. The table was constructed using a Factor of 10, however, the table is somewhat universal and speeds for Factors other than 10 are easily found. Simply multiply the given speeds in Table A.1 by the value 10/new Factor to obtain the new speeds.

Table A.1. Anaheim Indexers Rate Number/Speed Cross Reference

Base or Maximum Rate Number	Pulses Per Second (PPS)	Speed				
		X (mm/s) PPS/16	Y (mm/s) PPS/34	Z (mm/s) PPS/70	R (deg/s) PPS/34	T (deg/s) PPS/70
1	111.5	7.0	3.3	1.6	3.3	1.6
10	115.4	7.2	3.4	1.6	3.4	1.6
20	120.0	7.5	3.5	1.7	3.5	1.7
30	125.0	7.8	3.7	1.8	3.1	1.8
40	130.4	8.2	3.8	1.9	3.8	1.9
50	136.4	8.5	4.0	2.0	4.0	2.0
60	142.9	8.9	4.2	2.0	4.2	2.0
70	150.0	9.4	4.4	2.1	4.4	2.1
80	157.9	9.9	4.6	2.3	4.6	2.3
90	166.7	10.4	4.9	2.4	4.9	2.4
100	176.5	11.0	5.2	2.5	5.2	2.5
110	187.5	11.7	5.5	2.7	5.5	2.7
120	200.0	12.5	5.9	2.8	5.9	2.8
130	214.3	13.4	6.3	3.1	6.3	3.1
140	230.8	14.4	6.8	3.3	6.8	3.3
150	250.0	15.6	7.4	3.6	7.4	3.6
160	272.7	17.0	8.0	3.9	8.0	3.9
170	300.0	18.8	8.8	4.3	8.8	4.3
180	333.3	20.8	9.8	4.8	9.8	4.8
190	375.0	23.4	11.0	5.4	11.0	5.4
200	428.6	26.8	12.6	6.1	12.6	6.1
210	500.0	31.3	14.7	7.1	14.7	7.1
220	600.0	37.5	17.6	8.6	17.6	8.6
230	750.0	46.9	22.1	10.7	22.1	10.7
240	1000.0	62.5	29.4	14.3	29.4	14.3
250	1500.0	93.8	44.1	21.4	44.1	21.4
255	2000.0	125.0	58.8	28.6	58.8	28.6

## APPENDIX B

### SYSTEM IDIOSYNCRASIES

This appendix serves to alert the reader to the idiosyncrasies inherent to the present system, and gives solutions to each where applicable.

Idiosyncrasies inherent to the Octoson® which became apparent during this study include:

- 1) The video display locking up or fading completely.
- 2) The front panels of the console become totally nonfunctional.
- 3) The system powers on in a locked up state and never completes its initialization.
- 4) The stepper motors lose synchronization.

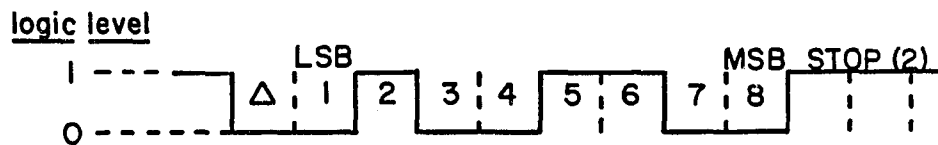
Ausonics Corporation assures that these problems are not particular to the unit at this site. However, Ausonics alluded to the fact that this unit went through an upgrade from all analog circuitry to include both analog and digital circuitry, and because of this may be susceptible to more frequent occurrences of these problems.

To recover from a loss of motor synchronization, an initialization usually suffices. However, to recover from all other problems a power off/on sequence, or a series of power off/on sequences, is required.

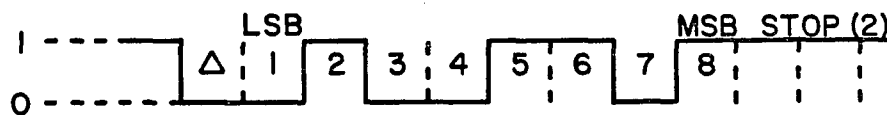
If the Anaheim Indexers fail to drive the motors, either of two problems may be the cause. First, the indexer power switch may have been in the on position when the Octoson® was powered on. The power transients caused by the Octoson® during power on may cause the indexers to power on improperly if their switch was on. A simple power off/on sequence of the indexers will correct this. To prevent this, ensure that the indexer power switch is in the off position prior to powering on the Octoson®.

Secondly, the data format of the Apple IIe may not be compatible with the indexers. The indexers require the following bit pattern: eight data bits, two stop bits, and no parity, with the most significant bit (MSB) of the eight data bits set to a low logic level. However, with the Apple IIe configured for eight data bits, the MSB is at a high logic level. Through software the Apple IIe is configured for seven data bits, two stop bits, and one parity bit always set to a low logic level (space parity). Because the indexers expect no parity, the space parity bit "tricks" the indexers into interpreting this as the MSB of eight data bits. This is illustrated in Figure B.1.

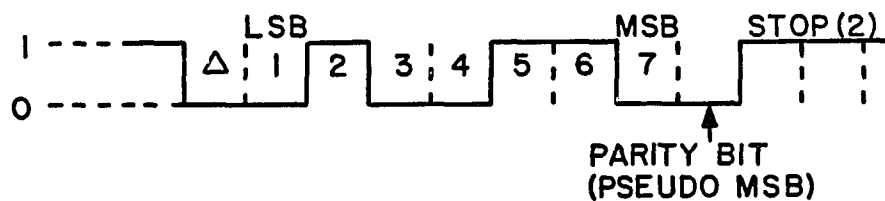
# DATA FORMAT REQUIRED BY INDEXERS



## APPLE II<sub>e</sub> DATA FORMAT WHEN USING 8 DATA BITS



## APPLE II<sub>e</sub> DATA FORMAT WHEN USING 7 DATA BITS AND SPACE PARITY



$\Delta$  START BIT

Figure B.1. Data Format of the Anaheim Indexer RS 232 Interface



## APPENDIX C

### SUMMARY OF RESULTS OF IN VIVO EXPERIMENTS

The modified system has been used successfully in approximately 30 experiments on dogs in an attempt to determine its feasibility as a hyperthermia device. The results were recently presented by Hynynen, et. al. [13,14], and are summarized here only for completeness.

The major result is that the system is capable of elevating the temperature of normal tissue to a therapeutically useful level. The maximum depth at which therapeutic temperatures can be achieved is still being investigated. However, at depths of at least 10 centimeters therapeutically useful temperatures were obtained, without the need for cooling the skin.

Another major result is that the average temperature during treatment may not be a good indication of the actual thermal dose the tissue receives. For long scanning times (i.e., the time it takes before energy deposition occurs again, or is refreshed), temperature fluctuations are large and the average temperature significantly underestimates the relative thermal exposure. Temperature fluctuations appear to increase as perfusion increases, therefore accentuating the difference between average temperature and thermal dose. Large temperature fluctuations may not be a problem, however, if they occur only inside the tumor volume.

On the other hand, if reduced temperature fluctuations are desired shorter scanning times (possibly smaller treatment volumes) would be needed. It is unclear at this time whether large temperature fluctuations are more or less efficacious than uniform temperature patterns for hyperthermia treatments.

## REFERENCES

1. Strohbehn, J.W., and Douple, E.B., "Hyperthermia and Cancer Therapy: A Review of Biomedical Engineering Contributions and Challenges," IEEE Transactions on Biomedical Engineering, Volume BME-31, Number 12, December, 1984, pp. 779-786.
2. Oleson, James R., "A Review of Magnetic Induction Methods for Hyperthermia Treatment of Cancer," IEEE Transactions on Biomedical Engineering, Volume BME-31, Number 1, January, 1984, pp. 91-97.
3. Stauffer, Paul R., Cetas, Thomas C., and Jones, Roger C., "Magnetic Induction Heating of Ferromagnetic Implants for Inducing Localized Hyperthermia in Deep-Seated Tumors," IEEE Transactions on Biomedical Engineering, Volume BME-31, Number 2, February, 1984, pp. 235-251.
4. Cheung, Augustine Y., and Neyzari, Ali, "Deep Local Hyperthermia for Cancer Therapy: External Electromagnetic and Ultrasound Techniques," Cancer Research, Volume 44, Number 10, October, 1984, pp. 4736s-4744s.
5. Turner, Paul F., "Regional Hyperthermia with an Annular Phased Array," IEEE Transactions on Biomedical Engineering, Volume BME-31, Number 1, January, 1984, pp. 106-114.
6. Hagmann, Mark J., Levin, Robert L., and Turner, Paul F., "A Comparison of the Annular Phased Array to Helical Coil Applicators for Limb and Torso Hyperthermia," IEEE Transactions on Biomedical Engineering, Volume BME-32, Number 11, November, 1985, pp. 916-927.
7. Hagmann, Mark J. and Levin, Ronald L., "Coupling Efficiency of Helical Coil Hyperthermia Applications," IEEE Transactions on Biomedical Engineering, Volume BME-32, Number 7, July, 1985, pp. 539-540.
8. Ruggera, Paul S., and Kantor, Gideon, "Development of a Family of RF Helical Coil Applicators Which Produce Transversely Uniform Axially Distributed Heating in Cylindrical Fat-Muscle Phantoms," IEEE Transactions on Biomedical Engineering, Volume BME-31, Number 1, January, 1984, pp. 98-105.

9. Stauffer, Paul S., Cetas, Thomas C., Fletcher, Anne E., DeYoung, Donald W., Dewhirst, Mark W., Oleson, James R., and Roemer, Robert B., "Observations on the Use of Ferromagnetic Implants for Inducing Hyperthermia," IEEE Transactions on Biomedical Engineering, Volume BME-31, Number 1, January, 1984, pp. 76-90.
10. Lele, P.P., "Hyperthermia by Ultrasound," Proceedings International Symposium on Cancer Therapy by Hyperthermia and Radiation, pp. 168-178, Washington, D.C., 1975.
11. Dickinson, Robert J., "An Ultrasound System for Local Hyperthermia Using Scanned Focussed Transducers," IEEE Transactions on Biomedical Engineering, Volume BME-31, Number 1, January, 1984, pp. 120-125.
12. Ocheltree, Kenneth B., Benkeser, Paul J., Frizzel, Leon A., and Cain, Charles A., "An Ultrasonic Phased Array Applicator for Hyperthermia," IEEE Transactions on Sonics and Ultrasonics, Volume SU-31, Number 5, September, 1984, pp. 526-531.
13. Hynynen, Kullervo, Roemer, Robert B., Johnson, Charles A., Moros, Eduardo, and Anhalt, Dennis P., "Temperature Fluctuations During Scanned Focussed Ultrasound Hyperthermia," Proceedings of the American Society of Mechanical Engineers, Winter Annual Meeting, Miami Beach, Florida, 1985.
14. Hynynen, Kullervo, Roemer, Robert B., Johnson, Charles A., Moros, Eduardo, and Anhalt, Dennis P., "The Effect of Scanning Speed on Temperature and Equivalent Thermal Exposure Distributions During Ultrasound Hyperthermia In Vivo," accepted for publication in the IEEE Transactions on Microwave Theory and Technology magazine, May, 1986.